The Time Dependent Spectral Emission of Proton Bombarded Aerogels

E. W. Marsh

A Thesis Submitted to the Department of Physics of the University of Arizona
in partial fulfillment of the requirements for the graduate degree of

Master of Science

in Physics

Thesis Director: W. S. Bickel

1997

REPORT DOCUMENTATION PAGE

Form Approved
OMB No. 0704-0188

1. AGENCY USE ONLY *(Leave blank)*

2. REPORT DATE
4 August 1998

3. REPORT TYPE AND DATES COVERED

4. TITLE AND SUBTITLE
THE TIME DEPENDENT SPECTRAL EMISSION OF PROTON BOMBARDED AEROGELS

5. FUNDING NUMBERS

6. AUTHOR(S)
E.W. Marsh

7. PERFORMING ORGANIZATION NAME(S) AND ADDRESS(ES)
University of Arizona

8. PERFORMING ORGANIZATION REPORT NUMBER
98-039

9. SPONSORING/MONITORING AGENCY NAME(S) AND ADDRESS(ES)
THE DEPARTMENT OF THE AIR FORCE
AFIT/CIA, BLDG 125
2950 P STREET
WPAFB OH 45433

10. SPONSORING/MONITORING AGENCY REPORT NUMBER

11. SUPPLEMENTARY NOTES

12a. DISTRIBUTION AVAILABILITY STATEMENT
Unlimited distribution
In Accordance With AFI 35-205/AFIT Sup 1

12b. DISTRIBUTION CODE

13. ABSTRACT *(Maximum 200 words)*

14. SUBJECT TERMS

15. NUMBER OF PAGES
82

16. PRICE CODE

17. SECURITY CLASSIFICATION OF REPORT	18. SECURITY CLASSIFICATION OF THIS PAGE	19. SECURITY CLASSIFICATION OF ABSTRACT	20. LIMITATION OF ABSTRACT

TABLE OF CONTENTS

List of Figures

ABSTRACT

The University of Arizona 2 MV Van de Graaff accelerated 1 MeV protons to bombard aerogel targets. The spectroscopic emission characteristics of proton bombarded aerogels 1.68 mm - 5.50 mm thick were studied, particularly the emission as a function of bombardment time. It was discovered that the intensities of proton bombarded aerogel emissions depend on proton beam current, emitted wavelength, aerogel thickness, observation position inside of the gel, the time the aerogel is bombarded in a particular experiment, the time the aerogel had been bombarded prior to an experiment, and the time elapsed between experiments. Increasing the current gives a higher emission, but the intensity is not directly proportional to current. Thicker aerogels are less affected by beam current changes. The spectrum ($\bar{\lambda}$3500 - 7000 $\mathring{A}$) from an aerogel is a continuum, reaching a maximum in the range λ4300 - 5300 $\mathring{A}$. The maximum is red shifted as current is increased and blue shifted as bombardment time is decreased. When protons first make contact with an aerogel, a strong intensity peak is observed, which then decays to a near constant value. In general, proton bombarded aerogel emission decreases with time bombarded prior to an experiment and increases with the time elapsed between experiments. The front of an aerogel (where the protons first make contact with it) is the point of maximum intensity. The point of maximum intensity moves downstream from the front of the aerogel as bombardment time increases. Since no spectral lines of hydrogen were seen, we suspect that we need thinner and/or less dense aerogels, and higher proton energy. Luminescence is the most likely form of emitted radiation.

Chapter 1: Introduction to Proton Bombarded Aerogels

In this century, experimenters in physics have gathered a wealth of spectroscopic data by sending low energy beam particles through both gases and foils. Now, a new target, namely the *aerogel*, has added another dimension to spectroscopy. Little is known about the spectroscopic properties of the aerogel. Experiments have only recently begun on gels. I have continued these experiments and made improvements which show that aerogel emission from proton bombardment is a complex event. The intensity of the light emitted at particular wavelengths in the visible spectrum depends on the beam current, beam energy, the aerogel thickness, and most surprisingly, *how long the proton beam has bombarded the aerogel* and *the time elapsed since an aerogel was bombarded.* This paper reports how aerogel emission depends on the very first bombardment of an aerogel by the proton beam, on the initial[1] bombardment and then on the time (t_s) elapsed since the aerogel has been bombarded, the total time (t_p) the aerogel has been bombarded prior to an experiment, and the time (t_b) the gel is bombarded for an individual experiment.

As an introduction to beam-aerogel experiments, we will review beam-gas and beam foil experiments for comparison. In the 1960's beam-foil experiments were used to excite and measure the mean lives of various energy levels of atoms and ions of various elements. Accelerated beam particles (atomic and molecular ions) were sent through a thin foil (1000 $\mathring{A}$)--usually carbon. The transmitted particles travel at a constant speed and the intensity emitted by the excited beam was a function of wavelength. The location

[1] "First bombardment" is not the same as "Initial bombardment". First bombardment is when the gel has never been bombarded before. Initial bombardment is the first time the gel is hit in a particular experiment—the gel has been bombarded prior to the initial bombardment for a data scan.

of particles after the foil (at x = 0) could be related to time after excitation, from which decay rates of a particular excited level could be measured (Bashkin, 1968).

Beam-gas experiments, a precursor to beam-foil experiments, have a long history, dating back to the early to mid 1900's. For beam-gas experiments, the target chamber is a differentially pumped collision chamber filled with the desired gas. Various gas pressures could be selected, essentially enabling the production of an assortment of 'target thicknesses', however, pressure gradients between the gas cell and the upstream and downstream vacuum beam lines caused fringing effects at the entrance and exit aperture of the collision chamber. Hence, no precise t = 0 could be established for the excitation of a particular beam particle (Bashkin, 1968).

Beam-gel experiments (Figure 1) are similar to beam-foil and beam-gas experiments. The aerogel is locked into the position that formerly held the foil. The aerogel is an extremely light solid—essentially a 'stretched out foil' or a 'high pressure' gas that is frozen in 'time and space'. Therefore, a gel could possibly exhibit spectral characteristics similar to both foils and gases. This possibility and the properties of aerogels used in our experiments will be discussed in detail later.

Chapter 2: Description of Problem/Time Dependence

The previous study of the time dependent emission features of proton bombarded aerogels has been limited. R. Morrison (1995) noted that when the ions of a proton beam (and other hydrogen beams) initially and abruptly entered an aerogel, the amount of light

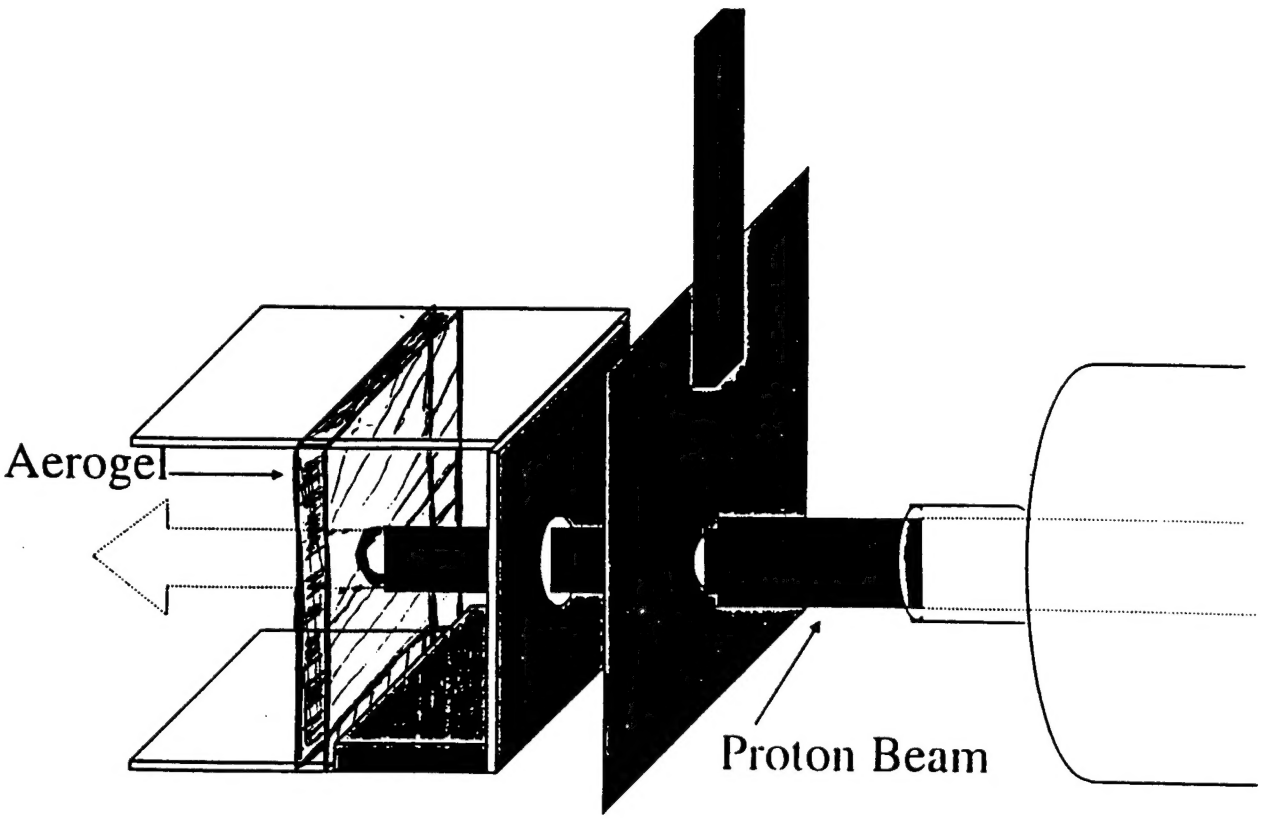

Figure 1: Proton Beam Bombarding an Aerogel

increased dramatically. We improved Morrison's technique for shutting the beam on and off rapidly by building a solenoid operated 'flap' to open and close the beam aperture, thereby turning the beam current to the aerogel on and off in a short amount of time. The flap eliminated mechanical error and showed that the abrupt peak in light intensity caused by the proton beam's initial hit on the aerogel was a physical event, not an artifact. We could now investigate how the abrupt peak in light intensity depended on the following: Wavelength (λ) of radiation emitted from the aerogel, thickness (T) of the aerogel, proton beam current (i), the amount of time (t_p) the aerogel has been bombarded with the proton beam prior to a data run, the amount of time (t_s) elapsed *since* the aerogel was last bombarded by the proton beam, time of bombardment (t_b) for a data scan, and from what part of the aerogel the emission occurs.[2] The flap mechanism is shown in Figure 2.

The flap opens and closes in a few milliseconds, about 2 orders of magnitude shorter than the time (0.0125 to 0.25 seconds) it takes our data acquisition system to take one data point. Therefore, the flap is either open or closed when data is being taken, not in between. The solenoid, which rotated the flap 90 degrees, was connected to a stepper motor to control the timing of the flap--its *duty cycle*[3]. The most common duty cycle was 1 (2.5 seconds open, 2.5 seconds closed), with other variations available.

---

[2] Example of (t_s), (t_p). (t_b).: If an aerogel's first bombardment is for 1 minute, then the beam current is turned off from the aerogel for 30 seconds, then bombarded again for 1 minute, (t_s) for the experiment would be 30 seconds. (t_p) would be 2 minutes, and (t_b) would be 1 minute for the first bombardment and 1 minute for the second.

[3] A duty cycle of ½ would equal to beam current on aerogel for x seconds, off for 2x seconds $= \frac{x}{2x}$

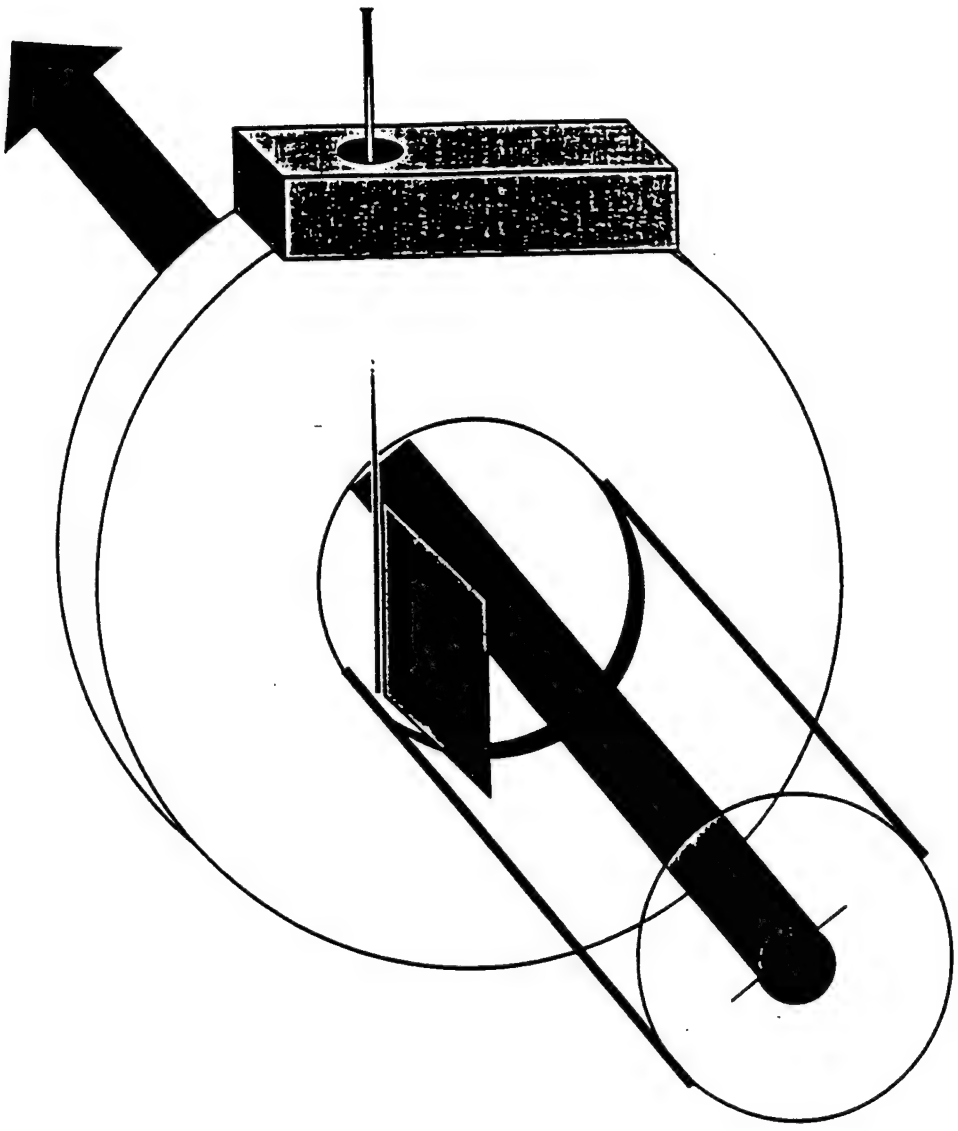

Figure 2: The Open Beam Flap (with Beam Inset)

Several experiments were performed, changing only one variable [of (λ), (T), (i), (t_p), (t_s), (t_b), and (x)] at a time while holding the others constant when possible[4].

A typical time dependent decay is shown in Figure 3. The y-axis is light intensity, the x-axis is time. The current is constant, but the light peaks when the beam first makes contact with the aerogel, then the light intensity decays. An explanation of terms is shown in Figure 4. Both the decay and the terms will be discussed in depth later.

Chapter 3: The Accelerator

The 2 MV UA Van de Graaff accelerator was used for the beam-aerogel experiments.

The Van de Graaff sends charged particles (hydrogen ions in these experiments) through a potential difference V to a final kinetic energy equal to the change in potential energy. Starting from Newton's second law.

$$F = ma = qE = \frac{qV}{d} \quad (1)$$

F = force (Newtons)

m = mass of particle accelerated (kg)

a = acceleration (m/s^2)

q = charge of particle accelerated (coulombs)

E = applied electric field (Volts/m)

V = potential difference (Volts) over a distance d (m). We also have,

[4] The term "if possible" is used because time bombarded cannot be held constant—only relative times of bombardment between gels can be compared

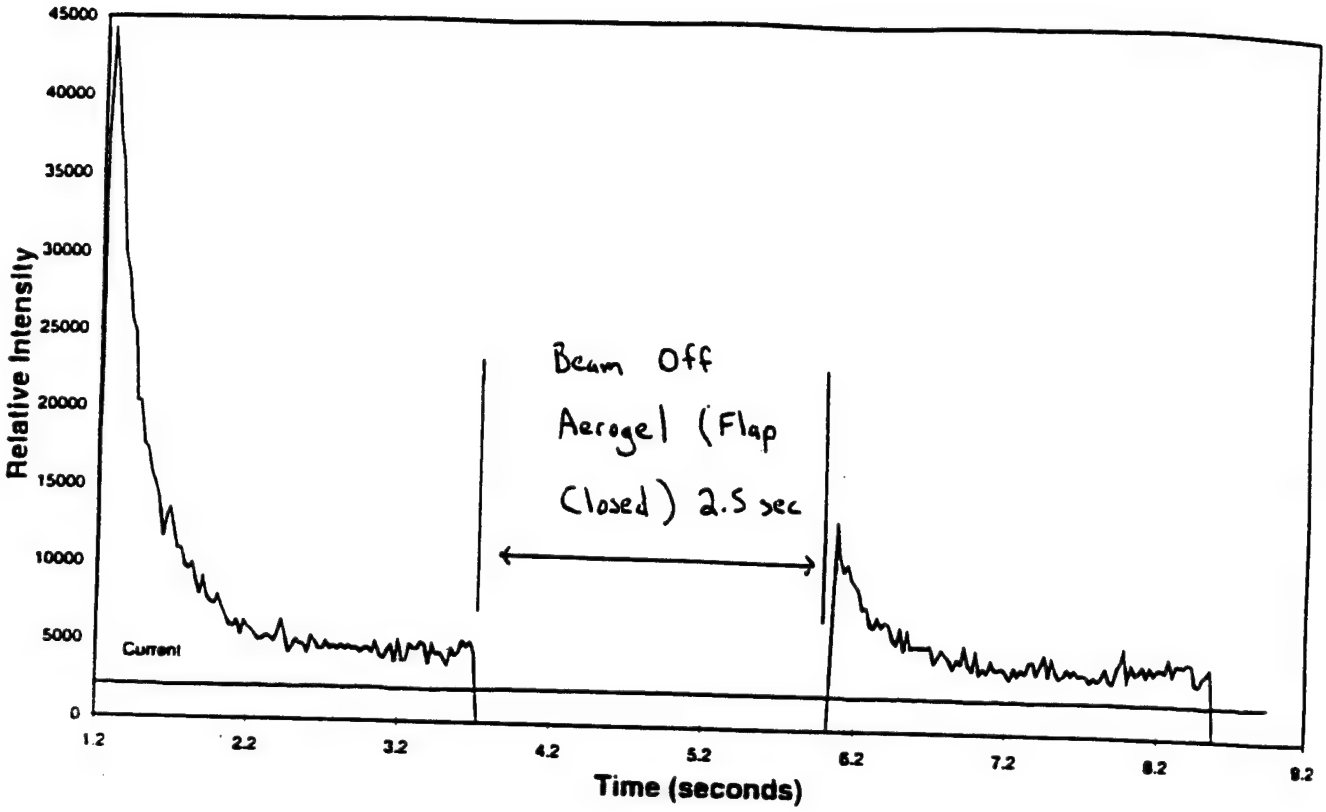

Figure 3: A Typical Time Dependent Decay

Duty Cycle = 1

$$\frac{\text{beam on aerogel 2.5 seconds}}{\text{beam off aerogel 2.5 seconds}}$$

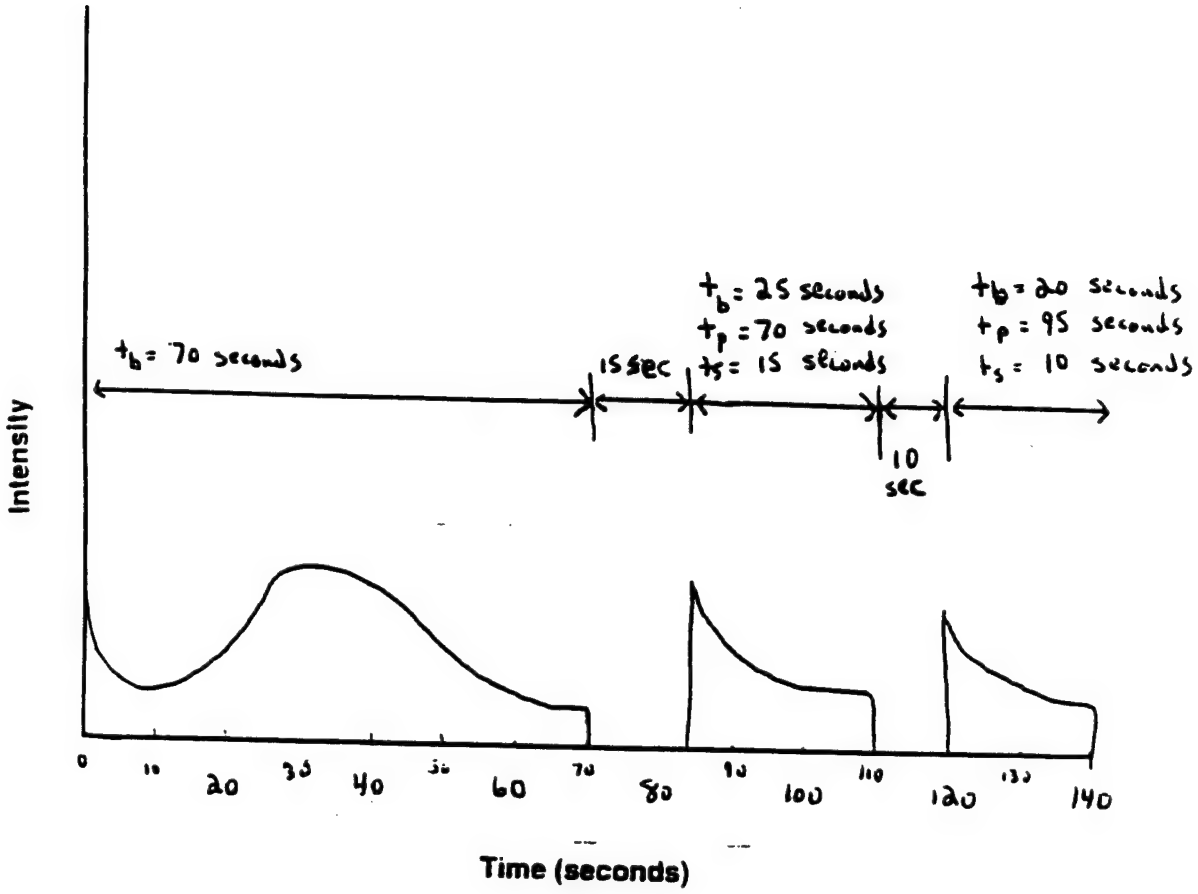

Figure 4: Definition of Terms--t_b, t_p, t_s

- t_b -- Time Bombarded for a Data Scan
- t_p -- Time Bombarded Prior to a Data Scan
- t_s -- Time Elapsed Since last Bombarded

$$v_f^2 = 2ad \qquad (2)$$

where v_f = final particle velocity (m/s), so

$$KE = \Delta PE$$
$$\frac{1}{2}mv_f^2 = qV \qquad (3)$$

In all experiments, the accelerating voltage is 1.0 MeV ± 50 KeV, giving nominally 1.0 MeV protons (with particle velocities of $1.4 * 10^7$ $^m/_s$). Hydrogen gas is extracted from a gas bottle into the ion source. The hydrogen gas molecules are ionized by two RF antennae which set up a 600 Hz radio frequency sinusoidal electric field inside. The antennae create oscillating electrons which will hit the atoms and molecules, ionizing them. The positively charged voltage at one end of the source sends ions the opposite direction out of the proton source exit channel down the accelerator tube under high vacuum (Model AN-2000, n.d.).

The ions ejected from the ion source are focused by a large positively charged ring which acts as a lens, creating a beam and directing all hydrogen ions to a point on the target at some selected place farther downstream. This process is shown in Figure 5.

A magnetic field directs the beam into one of 18 beam pipes that are angled from the center beam. The motion of the particle through the magnetic field can be calculated by equating the Lorentz force to centripetal force.

$$F = Bvq = \frac{mv^2}{r} \qquad (4)$$

B = magnetic field strength (Newtons-sec / coulombs-meters = Tesla = 10^4 Gauss)

Ejected Protons are Focused Downstream

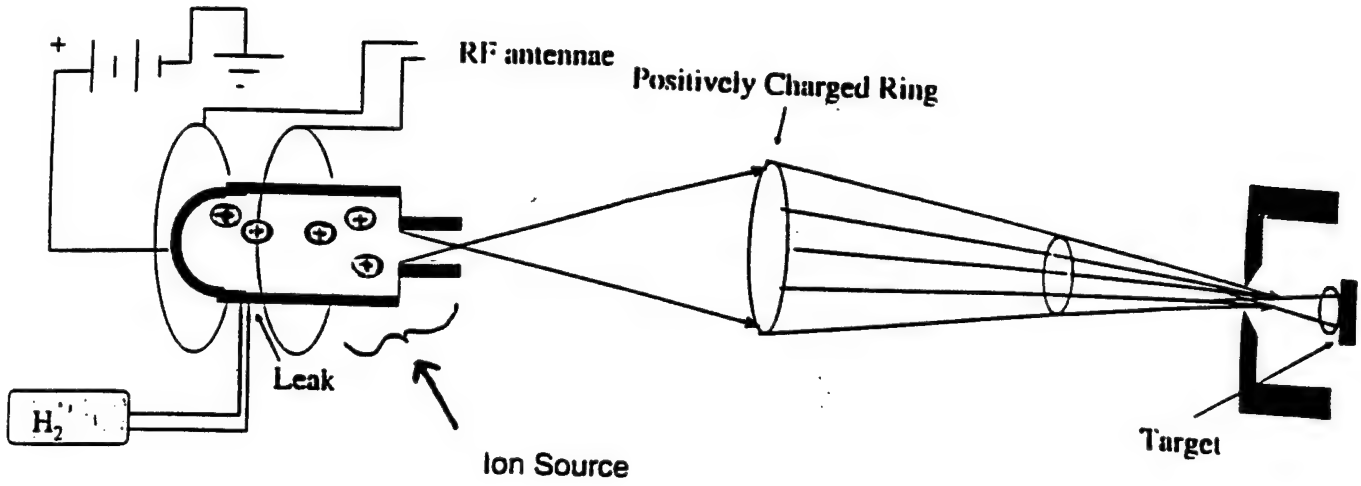

Figure 5: Gas Bottle, Ion Source, Antennae, and Focusing Ring

r = the radius charged particle in the magnetic field (m)

A Spectromagnetic Bending Magnet with a mass-energy product of 600 was used to direct hydrogen ions into the target chamber. Three different hydrogen beams were ejected from ion source: H^+ (protons), H_2^+, H_3^+. Protons were used in these experiments. Pressure for the experiments was kept in the range 1.2 to 1.8 * 10^{-6} torr.

Chapter 4: The Target Chamber

At the end of the beam pipe, a target chamber initially built by S. Bashkin was set up. This chamber was specifically modified by D. Manuszak for her Senior Honors Thesis at the University of Arizona. The chamber was set up as in Figure 6.
Inside the target chamber, a rotating wheel holds four aerogels and has four open holes to permit the beam to pass through and be measured in a shielded and suppressed Faraday cup positioned behind the rotating wheel. The beam current is also measured and monitored by a small collector located in the beam pipe just before the beam contacts the aerogel. This measurement ensured that the beam current was constant during all data acquisition, whereas the Faraday cup measured exact beam current.

Chapter 5: The External Optics and Photomultiplier (PM) Tube

Light emitted by the aerogel was collected by a concave mirror and directed to the entrance slit of a spectrometer, and finally collected in a photomultiplier (PM) tube.

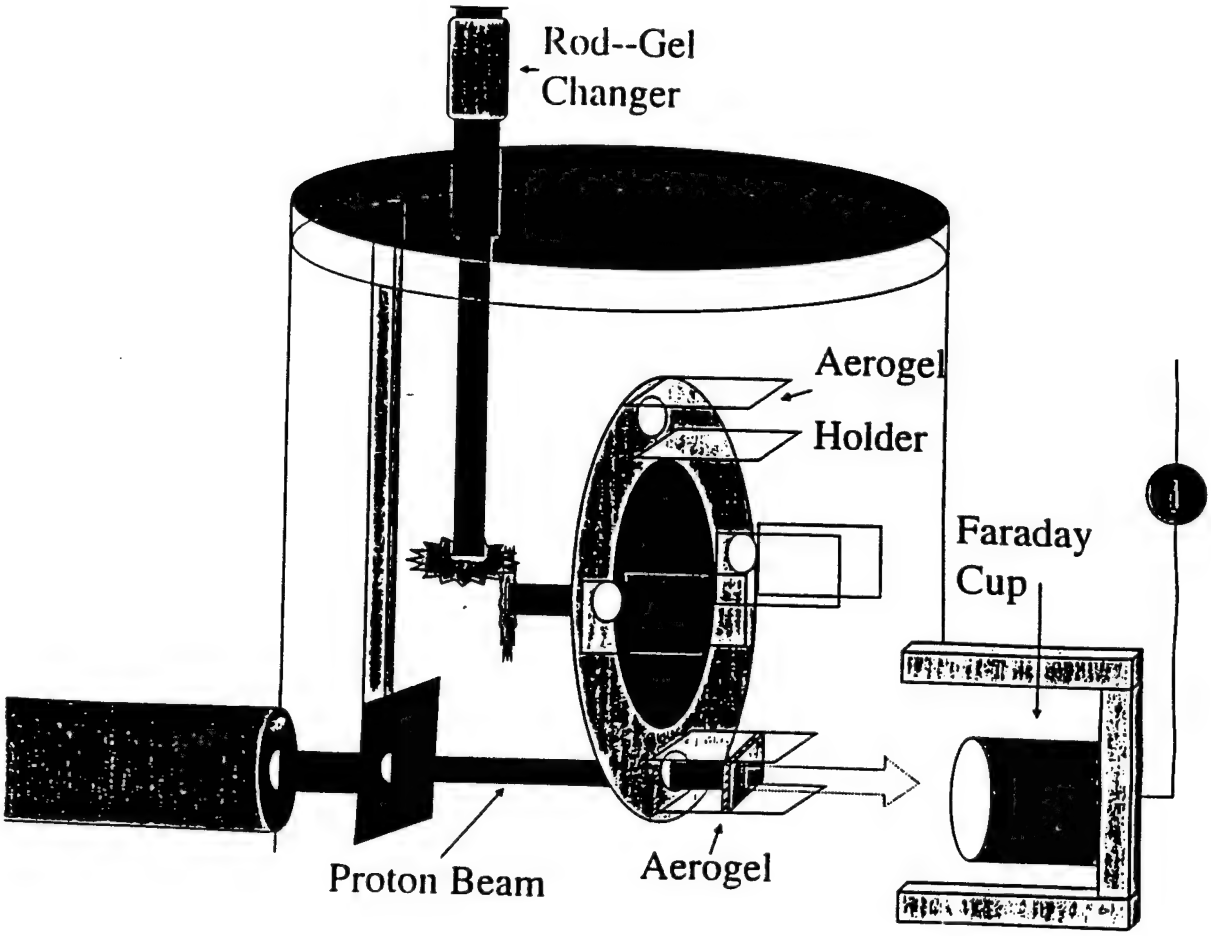

Figure 6: Target Chamber Set Up

The Spectrometer is a Heath EU-700 Scanning Monochromator—a single pass Czerny-Turner with folding mirrors that give the entrance and exit slit a common optical axis. It has resolution of 1 Å in the visible, a reciprocal dispersion of 20 Å /mm with a 1180 lines/mm grating. The slit width can be adjusted from 5 to 2000 μm. The slit height was set at 5 mm. It scans wavelengths ranging from λ1900 - 10000 Å at scan rates ranging from 0.05 to 20 Å /sec (Scanning Monochrometer, 1979). The target chamber, optical system, spectrometer, and PM assembly is shown in Figure 7.

The spectrometer focuses the image of the entrance slit onto the exit slit. The light from the aerogel enters the spectrometer through the entrance slit, which is at the focal point of the collimating mirror. The light reflects off plane mirror #2 to the collimating mirror, which reflects parallel light to the diffraction grating. Parallel light from the grating hits the focusing (camera) mirror, it reflects light to plane mirror #3, focusing the light on the exit slit. As the diffraction grating rotates, different wavelengths are focused at the exit slit and pass through it into a photon detector.

The photon detector is a RCA Model 1P21-2 photomultplier (PM) tube, number 2-T06950A. Maximum operating voltage is 900 Volts DC. Its operating wavelength range is 2000 - 8000 Å . The PM signal output pulses were amplified in a Tennelec Model TC 214 Linear Amplifier and Signal Channel Analyzer and sent to an IBM compatible computer.

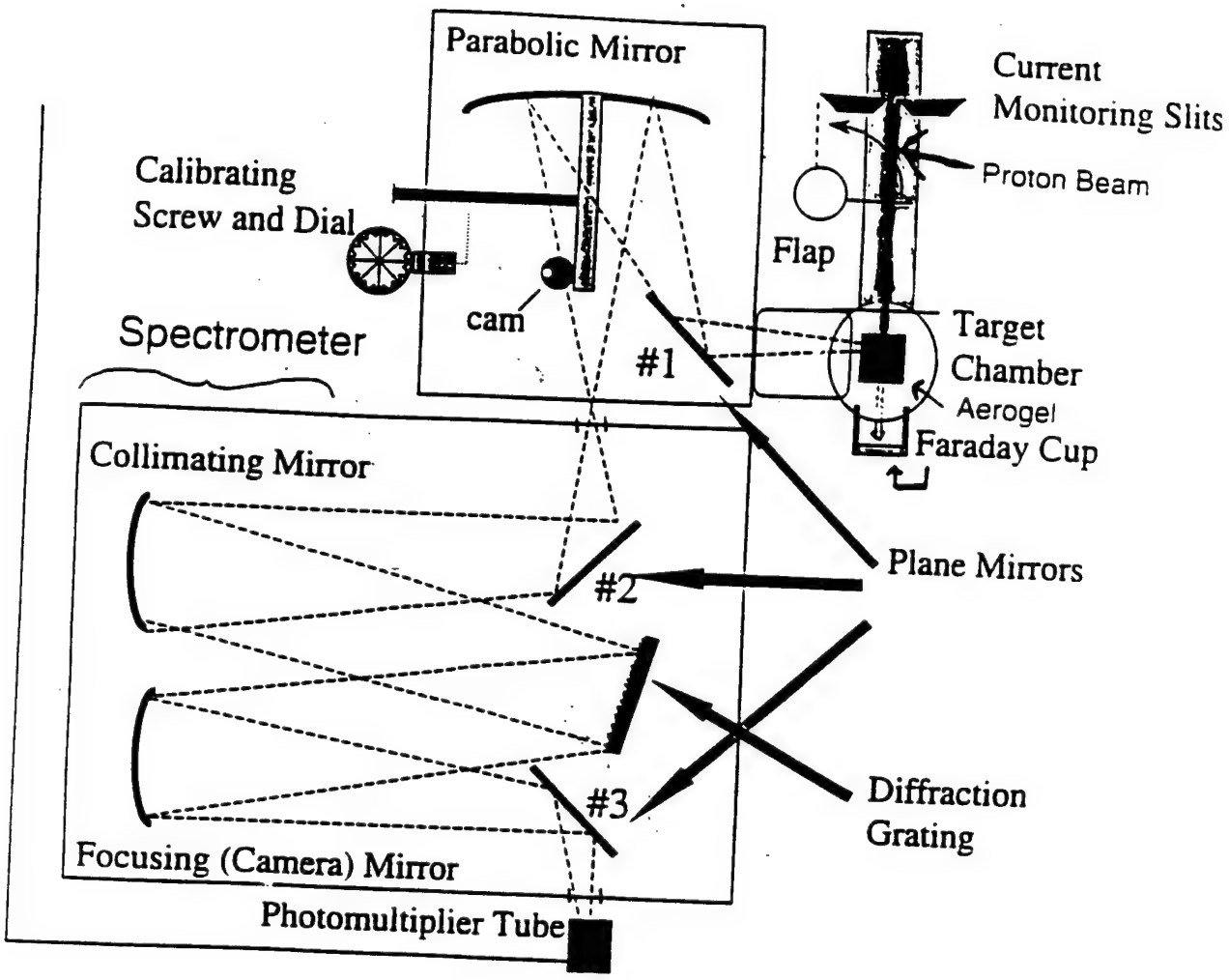

Figure 7: The Target Chamber, Optics and Spectrometer

Chapter 6: Data Acquisition System

The computer program *Snap Master*, which operated a pulse counting board, was used for data acquisition (HEM Data, 1994). Both intensity of light emitted from the aerogel (photon pulse rate) as a function of time and beam current as a function of time are simultaneously recorded using this program. Because current fluctuations could affect light intensity, beam current data were taken during all measurements to monitor its constancy.

Chapter 7: Scanning the Aerogel

The external optics focus the entrance slit of the spectrometer directly in the middle of the aerogel and on the proton beam axis. The parabolic mirror (shown in Figure 7) can be rotated (manually or with a rotating cam powered by a motor) to sweep the spectrometer entrance slit image across the aerogel, i.e. to scan and collect light anywhere from the front to the back of the aerogel. The "front" is where the beam first makes contact with the aerogel after entering the target chamber and is denoted as $x = 0$ (mm). Sweeping the entrance slit image from the front toward the back of the aerogel will be denoted as moving downstream from the $x = 0$ position (i.e. at $x = 2$, the optics would be focusing the slit 2 mm downstream from the front of the aerogel). Figure 8 shows how the optics scan from the front to the back of the aerogel as the parabolic mirror rotates.

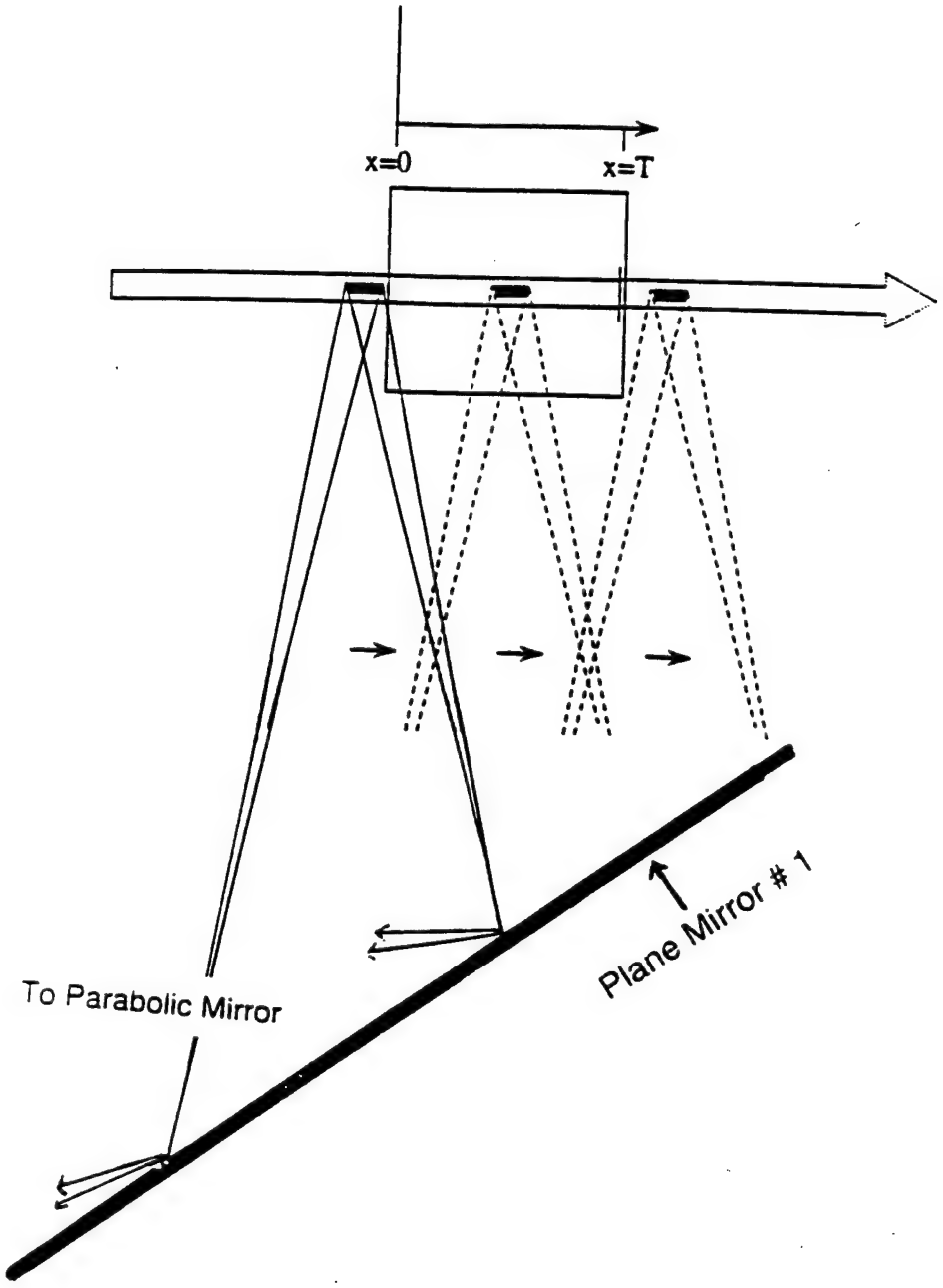

Figure 8: Scanning the Aerogel from x = 0 to x = T
(Top View)

Chapter 8: The Aerogel

Aerogels are solid, porous, transparent materials that can be made of silica, metal oxides, organic polymers and carbon (most commonly silica). Aerogel densities can be as low as 5 milligrams/cm^3. They can be formed into any shape and can be cut but are very delicate and easily crush between your fingers (Hunt 1). They have a refractive index of 1.01 to 1.02 in the visible. Aerogels can be as much as 99.5% porous and the pores in the aerogel range from 10 to 50 nanometers ("Aerogels", 1989).

Aerogels have an unusually low thermal conductivity. T_c for evacuated silica aerogels is 0.007 milliwatts / meter-Kelvin. In other words, an aerogel 2.5 cm thick has the same thermal resistance as a window of ten successive double panes of glass. It is expected that aerogels will commonly be used as insulators in refrigerators and windows (Hunt, 1995). Silica aerogels can be used as electrical insulators between computer chips, while carbon aerogels, with a higher dielectric constant, are being tested as capacitors (Wu, 1996). They have also been used as cosmic ray detectors. When entering an aerogel, high energy particles decelerate rapidly emitting visible light in the form of Cerenkov radiation (Anderson, 1991).

Our aerogels were made by first mixing an tetraethylorthosilicate (TEOS) and water[5]. Water reacts with the silicone and causes it to form pure silica particles. Alcohol is added to make TEOS and water miscible. Liquid catalysts are added—the silica particles link together in the aerogel form. Liquid CO_2 is added to the aerogel before it is heated in an autoclave to make its components pure silica ("Aerogels", 1989).

---

[5] Arlon Hunt, of the Lawrence Berkeley Laboratory, manufactured our aerogels. He has been developing and working with aerogels for 17 years.

The density of aerogels used in these experiments was 0.1 grams/ cm^3. The gels were cut into small rectangles about 1 cm square at the front face ranging from 1.68 mm to 5.50 mm thick.

The aerogel thickness was measured with a calipers that measure to 1/100 millimeter. These thickness measurements were confirmed by doing calibrations in the target chamber. A precisely measured piece of tantalum was set in the target chamber where the aerogel would be located. A dispersed light was positioned behind the small tantalum plate outside of the target chamber, providing a constant background light source. As the observation point was moved from the front to the back of the plate, light was collected and recorded. To scan from the front to the back of the tantalum plate, the parabolic mirror was rotated by turning the calibration screw at a rate of $\frac{1}{5}\frac{unit}{\text{sec}}$ (1 unit on the dial corresponded to moving the calibration screw 0.025 mm). The resultant intensity curve was an upside down trapezoid (expected from the convolution of the 1000 μm [1 mm] rectangular exit slit and the rectangular tantalum plate). The half width of each leg of the trapezoid determined the edge of the tantalum plate. This calibrated a distance (Δx) in the target chamber as a function of the distance the calibration screw was moved. The ratio is 0.21 mm in target chamber for every 1 unit on the dial. This corresponds to 8.4 mm in the target chamber for every 1 mm the calibration screw was moved. Plots of light intensity as a function of dial reading for the tantalum plate and the aerogel are shown in Figures 9 and 10. In Figure 9, a linear regression line is drawn through the data in order to get each leg of the trapezoid. In figure 10, the aerogel lets light pass through between 1.0 and 2.5 mm downstream of x = 0 mm, but lets no light through at the front and back.

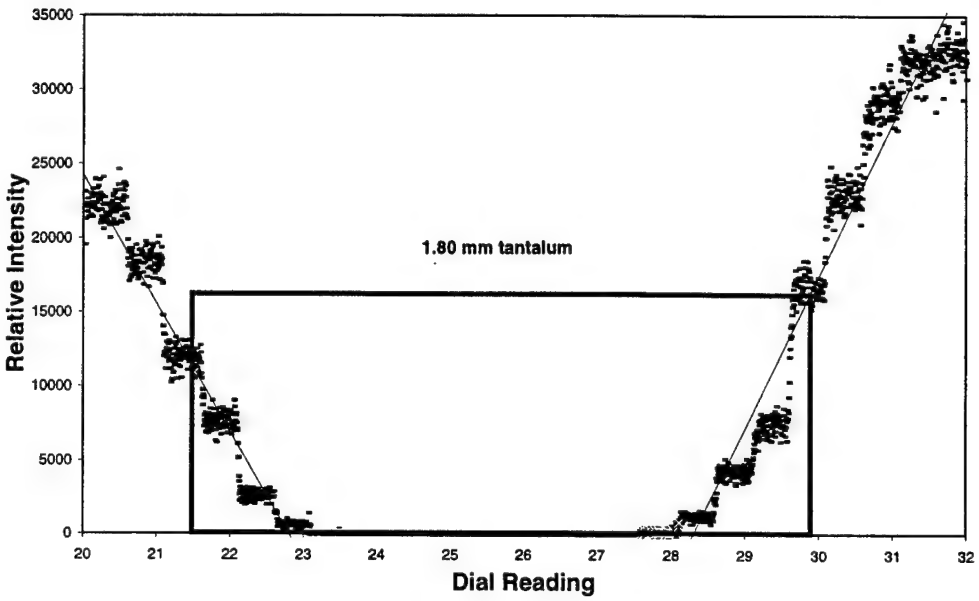

FIGURE 9: **LIGHT INTENSITY AS A FUNCTION OF DIAL READING FOR THE 'BACK-LIT' TANTALUM PLATE (CALIBRATED DISTANCE = 0.21 mm in target chamber/ 1 unit on Dial)**

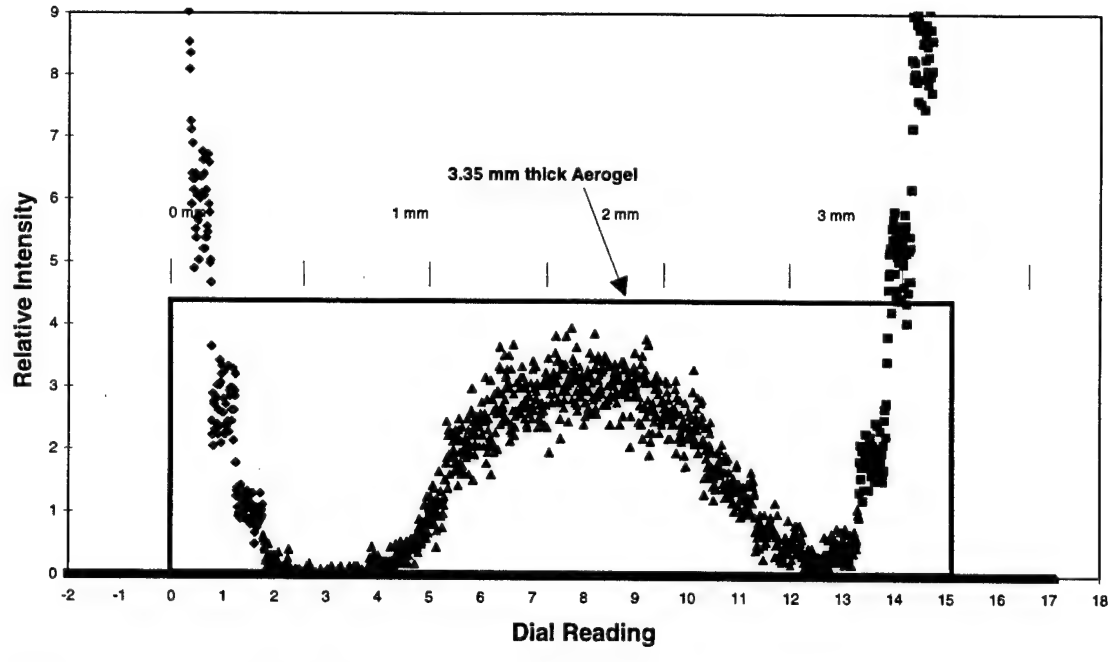

FIGURE 10: **LIGHT INTENSITY AS A FUNCTION OF DIAL READING FOR A 'BACK-LIT' AEROGEL**

Aerogels are essentially opaque at the edges when being back-lit. This is not the case when they are bombarded. Surprisingly, the location of maximum intensity during bombardment is the point at which the aerogel is opaque when it is back-lit!

Chapter 9: Procedure/Data Acquisition

We want to characterize the spectral and time dependent emission of light from aerogels. Since the emission of an aerogel depends upon many variables, the process of categorizing its emission becomes methodical. We proceeded as follows:

1. Visually observe (by eye) the aerogel as it is being excited.
2. Measure the spectra (λ 3500 -7000 Å) emitted by the aerogel during proton bombardment.
    a. Determine the emission as a function of wavelength.
    b. Search for spectral lines (i.e. The Balmer lines from hydrogen).
    c. Choose a fixed wavelength and observe the emission as a function of position in aerogel.
3. Collect data for many sweeps across the aerogel (scanning the aerogel) i.e. emission as a function of all positions x in the aerogel.
    a. Measure the emission.
    b. Search for spectral lines.

c. Determine how emission depends on: Wavelength (λ) emitted, aerogel thickness (T), beam current (i), position (x) in aerogel, beam particle energy (E), beam particle used (H^+, H_2^+, H_3^+).

4. Examine the time dependent features of aerogel emission.

a. Examine the very first bombardment of an aerogel--emission as a function of wavelength (λ) emitted and aerogel thickness (T).

b. Measure the spectra (λ 3500 -7000 Å) as a function of time bombarded for data run (t_b).

c. Measure aerogel emission as a function of time bombarded prior (t_p) for different (λ), (i), (T), and (x).

d. Measure Aerogel emission as a function of time bombarded since (t_s) for different (λ), (i), and (T).

All the above measurements were done, but the work for this thesis concentrated on Part 4, the time dependence of aerogel emission. Doing time dependent studies of aerogel emission is a very delicate process. In order to see how an aerogel reacts to the first bombardment of the proton beam hitting its surface, one must choose the wavelength to observe, the current, and all the other variables carefully. One can bombard the aerogel for the first time only once. The experiment cannot be repeated, unless a new aerogel is inserted.

Chapter 10: Observations and Data

VISUAL OBSERVATIONS

I. First Bombardment of Aerogel

The aerogel glows violet for 5-10 seconds the very first time it is bombarded. The color then changes to blue. As it is bombarded for longer times, the violet color seen when beam particles first enter the aerogel is gradually replaced by a blue glow.

II. Time Dependent Scans

During short term time dependent scans (i.e. using the beam flap to open and close the beam to and from the aerogel in times less than or equal to 10 seconds), it is visibly apparent that the aerogel produces more light when the beam particles initially bombard the aerogel than after the beam has been bombarding the aerogel for a few seconds (as in Figure 3).

III. Miscellaneous

During one experiment, the aerogel began to arc from the point of bombardment to the aerogel holder. The arcing line was red.

When an aerogel is taken out of the target chamber after an experiment, it has a slightly dark to virtually black coating on it at the point of ion bombardment. This darkening is due to carbon buildup on the front surface from cracking of the hydrocarbon pump oil which is part of the residual gas in the vacuum.

All visible wavelengths reveal time dependent features consisting of a sharp intensity spike that occurs from the initial bombardment of protons. In general, observations were made in the λ4000-5500 Å region because the emission intensity is highest there.

Time dependent spectral emission occurs in the aerogel from x = 0 to x = T. We measured mainly at the front of the aerogel because emission was strongest there.

No Balmer lines were seen in front of, inside, or behind the aerogel.

SCANS OF AN AEROGEL

I. Spectra and Scans across an Aerogel

Figure 11 shows the spectrum from a proton bombarded aerogel (proton energy = 1.0 MeV). The light intensity emitted from the aerogel as a function of wavelength is essentially a continuum. No spectral lines have yet been seen in an aerogel spectrum. This spectrum shows that the intensity maximum occurs at approximately 4500 Å . Figure 12 shows a scan over the aerogel from x = 0 to x = T. An intensity maximum occurs at the front of the aerogel, decreasing toward the back. This trend of a peak at the front of a aerogel, decreasing thereafter, was highly reproducible. This was a central topic of Manuszak's research.

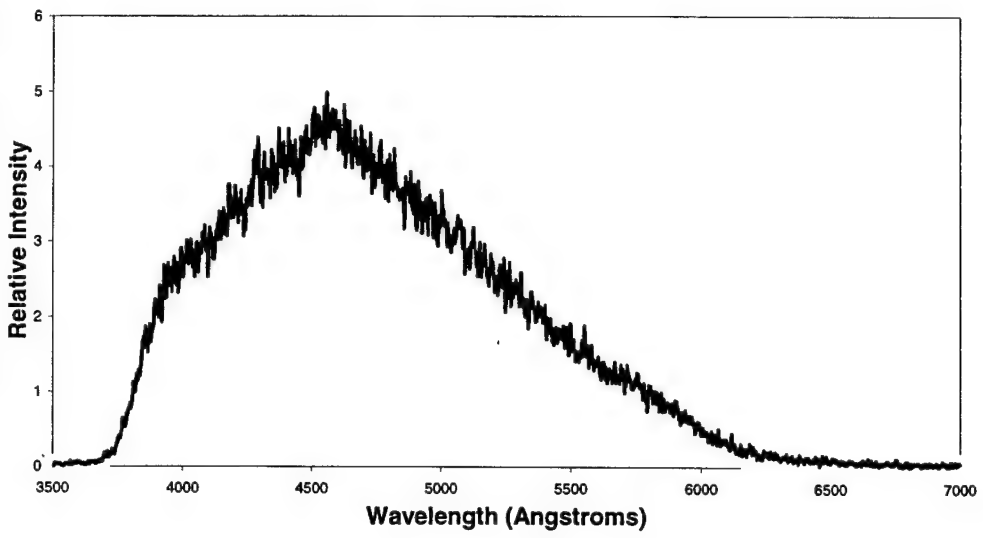

FIGURE 11: SPECTRAL SCAN (λ3500 TO 7000) WITH MAXIMUM NEAR 4500 Å

λ3500 - 7000 Å

i = 0.12 μA

T = 5.50 mm

II. CURRENT DEPENDENCE OF AEROGEL SPECTRA

Beam current dependence of aerogel emission has been explored in great detail in this paper. Figure 13 is a plot of two spectra (λ3500 to 7000 Å) of an aerogel, one spectrum taken at beam current 0.12 ± 0.005 μA, the other taken at 0.30 ± 0.005 μA (E = 1.0 MeV protons). The aerogel thickness is 5.50 mm. [6]

[6] Unless other wise noted, beam current variation is always ± 0.005 μA and **all particles are 1.0 MeV protons.**

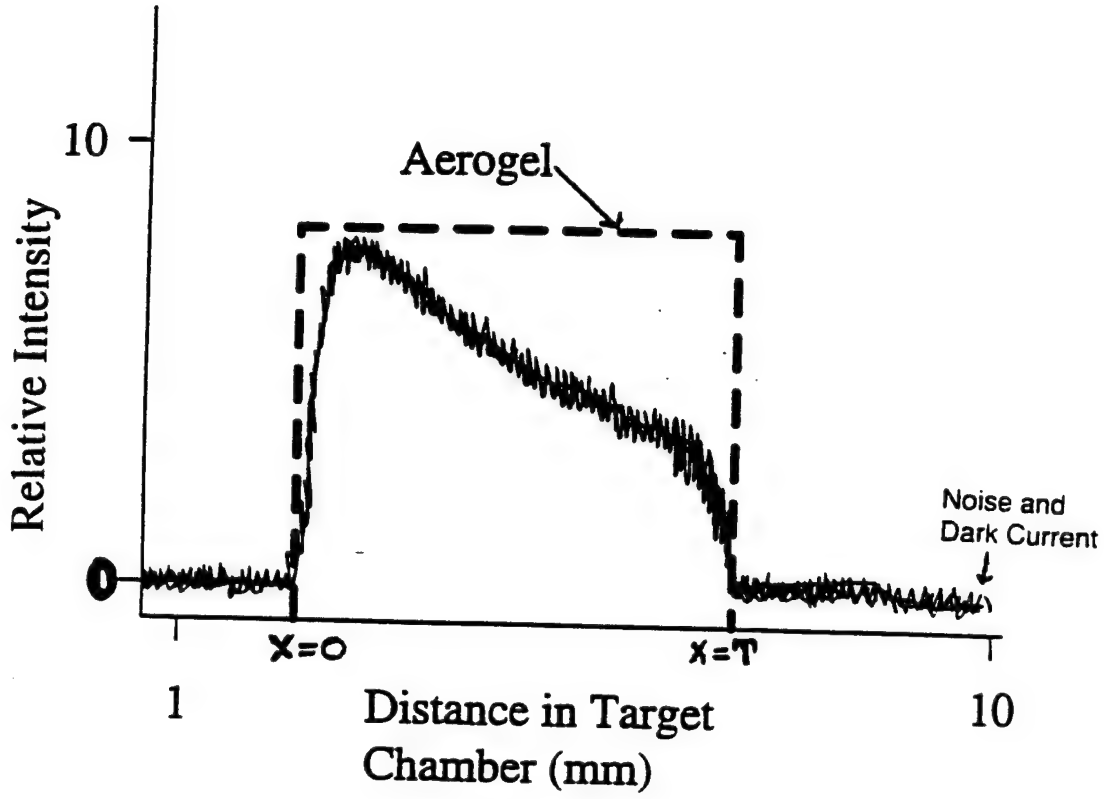

Figure 12: A Typical Scan Across an Aerogel
(Constant Current, Constant Wavelength)

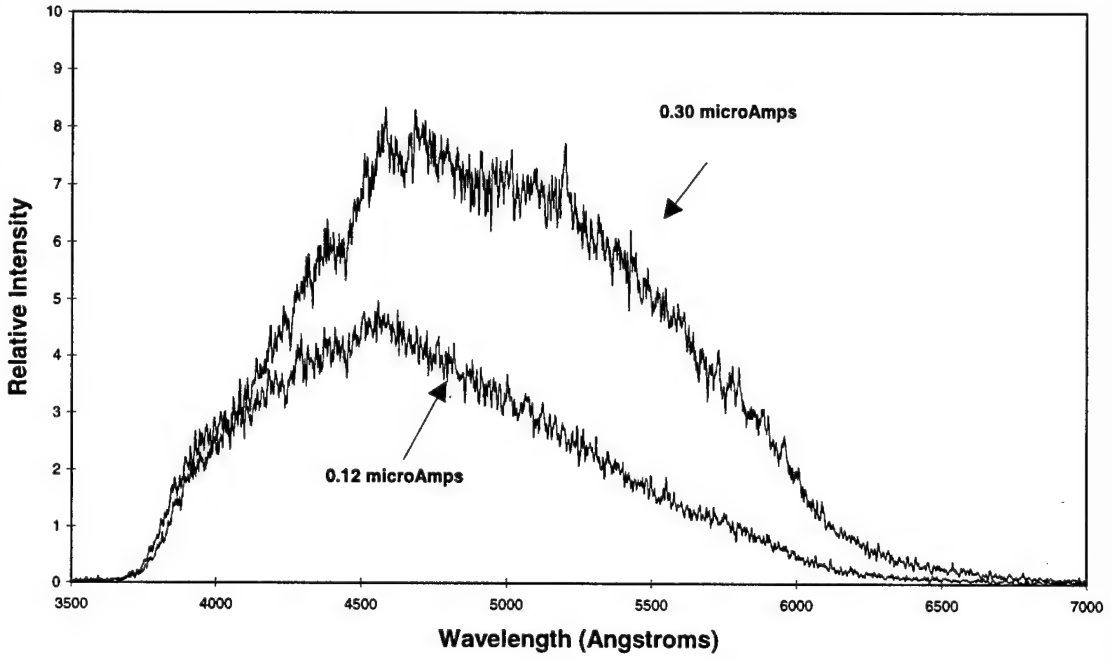

FIGURE 13: COMPARISON OF SPECTRA TAKEN AT TWO DIFFERENT CURRENTS

λ3500 - 7000 Å

T = 5.50 mm

The spectrum with the higher beam current has an intensity maximum at 4684 Å , while the spectrum with the lower beam current is a maximum at 4555 Å . This result is consistent with data from 3.56 mm and a 4.17 mm thick aerogels (Table 1). The shift of the spectral maximum may not be the most important characteristic of the spectra,

Table 1: Current Dependence of Aerogel Spectra

Aerogel (mm)	Current (μA)	Wavelength of Maximum (Angstroms)	Shift in Maximum (Angstroms)
3.56	0.14	4659	590
	0.28	5249	
4.17	0.12	4719	456
	0.32	5175	
5.50	0.12	4555	129
	0.30	4684	

but the change in the shape of the spectra is significant. Increasing the current often causes the emission to increase and red shifts the spectrum. While the spectrum from the 5.50 mm thick aerogel doesn't have a significant shift in its maximum with increasing current, the intensity at higher wavelengths are proportionally much larger for the higher current spectrum than for the lower current. This trend is seen in the other aerogels as well.

TIME DEPENDENT SCANS

I. First bombardment of Aerogels

Figure 14 shows the light intensity as a function of time for an aerogel that is being bombarded by protons for the very first time[7]. The intensity was measured for a long time (> 60 sec—a long term time dependent scan) after the initial bombardment[8].

[7] An experiment on an aerogel that has never been bombarded will be denoted as a first bombardment
[8] Long term scans, such as in figure 12, are defined as scans in which the beam bombards the aerogel for > 60 sec. Short term sequences are a number of identical short bombardments (1-10 seconds) on the aerogel.

The emission at λ4000 Å from the front of the aerogel (x = 0.50 mm) was measured where the maximum intensity occurs[9]. The beam current was 0.12 μA. The aerogel thickness is 3.58 mm.

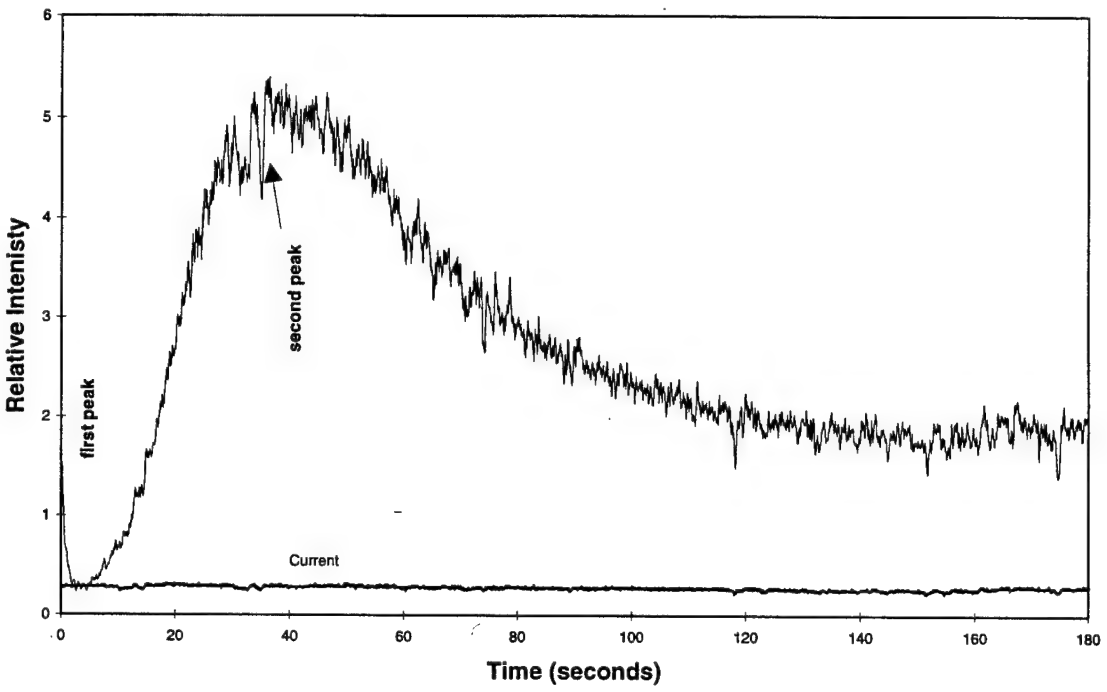

FIGURE 14: FIRST BOMBARDMENT OF AEROGEL

λ4000 Å

i = 0.12 μA

T = 3.58 mm

x = 0.50 mm

In Figure 14 , one sharp intensity peak occurs at initial bombardment (t = 0), while another intensity peak occurs 37.15 seconds into the scan. The relative intensity[10] of the

[9] The maximum intensity occurs in a region at the front of the gel defined by 0.50 mm +- 0.17 mm deep into the gel.

first peak is 1.6 and the second peak 5.5 for a ratio of 1 : 3.4. The long term intensity[11] reaches a constant value of 1.9. Table 2 shows data from fresh aerogel bombardments for comparison.

Table 2: Comparison of First Bombardments of Four Aerogels

Aerogel Thickness (mm)	**Wavelength Observed** (Angstroms)	**1st PEAK: Intensity @ Time** (Relative I @ seconds)	**2nd PEAK: Intensity @ Time** (Relative I @ seconds)	**Ratio** (1st peak: 2nd peak)	**Long term Intensity*** (Relative I)
1.68	4000	1.1 @ t = 0	2.5 @ t = 41.30	1 : 2.3	0.4
2.92	4000	1.0 @ t = 0	3.3 @ t = 30.70	1 : 3.3	1.0
3.58	4000	1.6 @ t = 0	5.5 @ t = 37.15	1 : 3.4	1.9
3.35	4500*	0.9 @ t = 0	8.4 @ t = 42.35	1 : 9.3	3.3

The one aerogel that was observed at 4500 Å (*) had the lowest initial peak, but it had a 2nd peak more than twice as large as the ones from the two thinnest gels and almost 1 1/2 times that from the thickest aerogel (see Table 2). This correlates with visual observations of the first bombardment of an aerogel, where the aerogel is seen to glow violet, then blue (i.e. 4000 to 4500 Å , a transition from the violet to the blue part of the spectrum).

There is a definite correlation between thickness of the aerogel and intensity of the 2nd peak, as well as thickness of the aerogel and long term intensity.

[10] Relative intensities are on a 1-10 scale. Comparisons of the relative intensities cannot be done for all scans reported. Relevant comparisons are noted by the author.

[11] The long term intensity is defined as the constant intensity of the gel for 60 seconds at the end of the 3 minute scan.

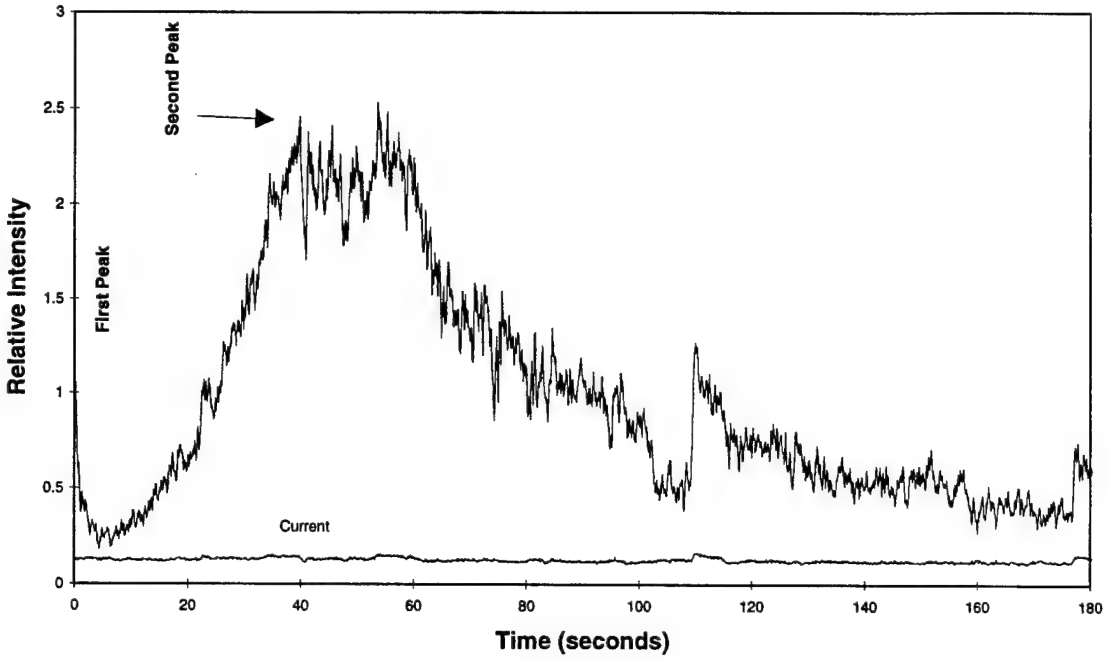

FIGURE 15A: **FIRST BOMBARDMENT OF AEROGEL**

λ4000 Å

i = 0.12 μA

T = 1.68 mm

x = 0.50 mm

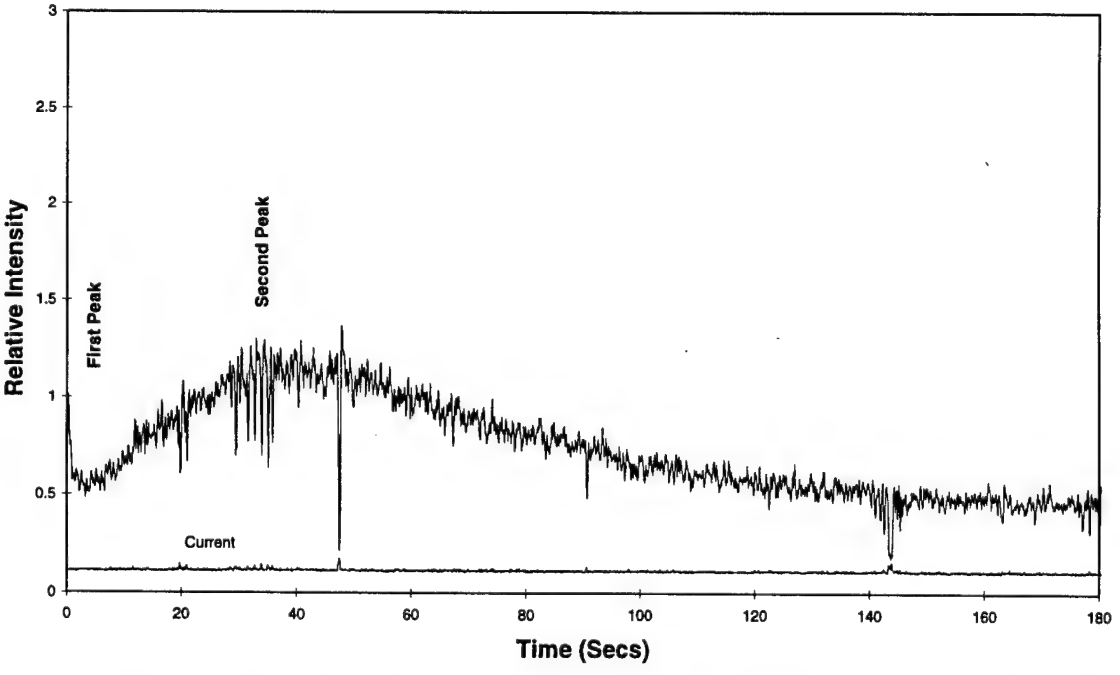

FIGURE 15b: **SECOND EVER BOMBARDMENT OF AEROGEL (Same conditions as 15b except Δt_b = 180 seconds)**

First bombardments give an intensity-time curve significantly different than any other time sequence. This is shown in Figures 15a and 15b. The experimental parameters that yielded the two curves were the same; the only variable that is changed is the time the beam has bombarded the aerogel prior ($t_p = 0$ for Figure 15a, $t_p = 180$ sec for Figure 15b). Figure 15a is the first bombardment scan, and Figure 15b is the scan taken directly after the first bombardment. Both are 3 minutes long, both are from the same 1.68 mm thick aerogel.

The curves are quite different. The emission from the very first bombardment of an aerogel cannot be duplicated. The initial peak intensity at t = 0 of the first bombardment is 1.1. The peak at t = 41.30 seconds is 2.5 (Figure 15a). The initial peak intensity at t = 0 for the second bombardment is 1.1. But, at t = 35 seconds it is only 1.5 (Figure 15b). Because two experiments done under identical conditions (except a change in time bombarded prior (t_p)) yield significantly different results, some evolution of the aerogel properties must be taking place. Figure 15a also shows that slight fluctuations in the current (as little as 0.02 μA, $^{\delta i}/_i$ = 20 % for 0.1 μA, 7% for 0.3 μA) can cause extreme changes (over 100%) in the emission from an aerogel.

II. Evolution of Aerogels

As seen in the previous figures, the aerogel emits light differently depending on whether it is being bombarded for the first time or has been bombarded previously, with all other variables held constant. The emission changes as the total time of bombardment

increases as well. In general, the emission degrades as a function of time bombarded prior (t_p). The first short term time dependent sequence is shown in Figure 16. The aerogel thickness is 3.85 mm. The current is 0.18 μAmps. The observation point is the front of the aerogel. The top curve (Figure 16) is the sum of 6 identical bombardments of 2.65 seconds length[12]. The bottom curve (Figure 16) is done under identical conditions except the aerogel had been bombarded for 105 seconds longer ($t_p^{bottom} = t_p^{top} + 105$ seconds). The six bombardments that were summed to get Figure 15 (top) are seen in succession in Figure 17 (as they would appear on the computer screen after data was acquired using the program *Snap Master*). The six bombardments are individually plotted in Figure 18 to show that the variation among them is small. Successive bombardments were only summed if variations between them were small.

Figure 16 shows that a prior bombardment time difference of 105 seconds can cause the intensity of the peak to drop by a factor of 3.5 (8.8 to 2.5). The end intensity[13] dropped by a factor of 2.5 (from 3.2 to 1.3). The results are surprising and significant. The amount of time an aerogel has been bombarded prior to an experiment has a significant affect on emission. This was consistently observed during many experiments. Results are shown for 4500 $\mathring{A}$ in Table 3.

[12] When bombardments are summed, the final curve is divided by the number of bombardments summed.
[13] The end intensity is similar to the long term intensity, except it is for short term scans. It is defined as the intensity at the end of a short term scan.

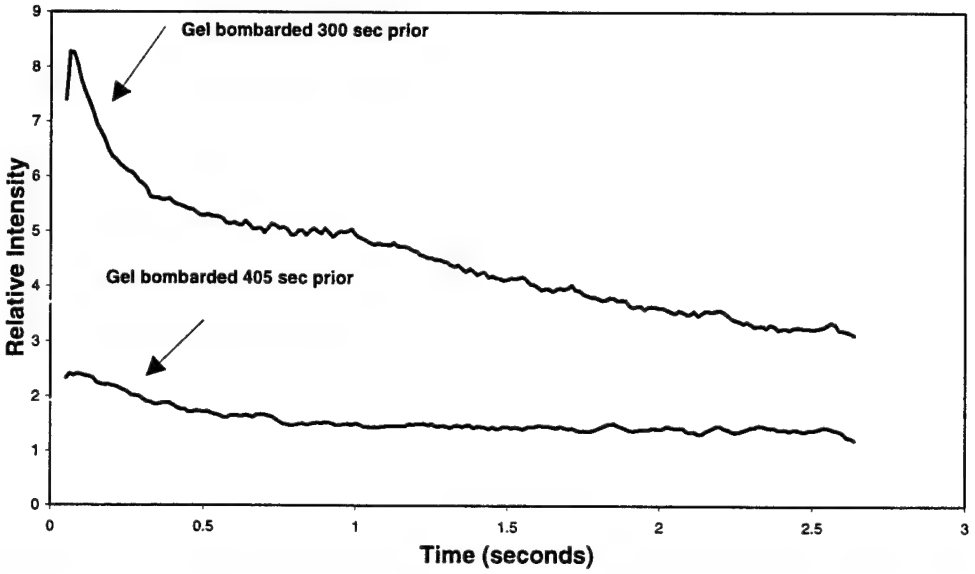

FIGURE 16: **COMPARISON OF TWO SHORT TERM TIME DEPENDENT SEQUENCES WITH t_p DIFFERENCE OF 105 SECONDS**

λ4000 Å

i = 0.18 μA

T = 3.85 mm

$\underline{\Delta t_p = 105 \text{ seconds}}$

x = 0.50 mm

Table 3:

Wavelength Scanned (Angstroms)	t_p for higher emission (seconds)	t_p for lower emission (seconds)	Time difference (seconds)	Multiplicative drop in Initial Intensity	Multiplicative drop in End Intensity
4000	300	405	105	3.5 x	2.5 x
4500	330*	442.5	102.5	1.8 x	3.3 x

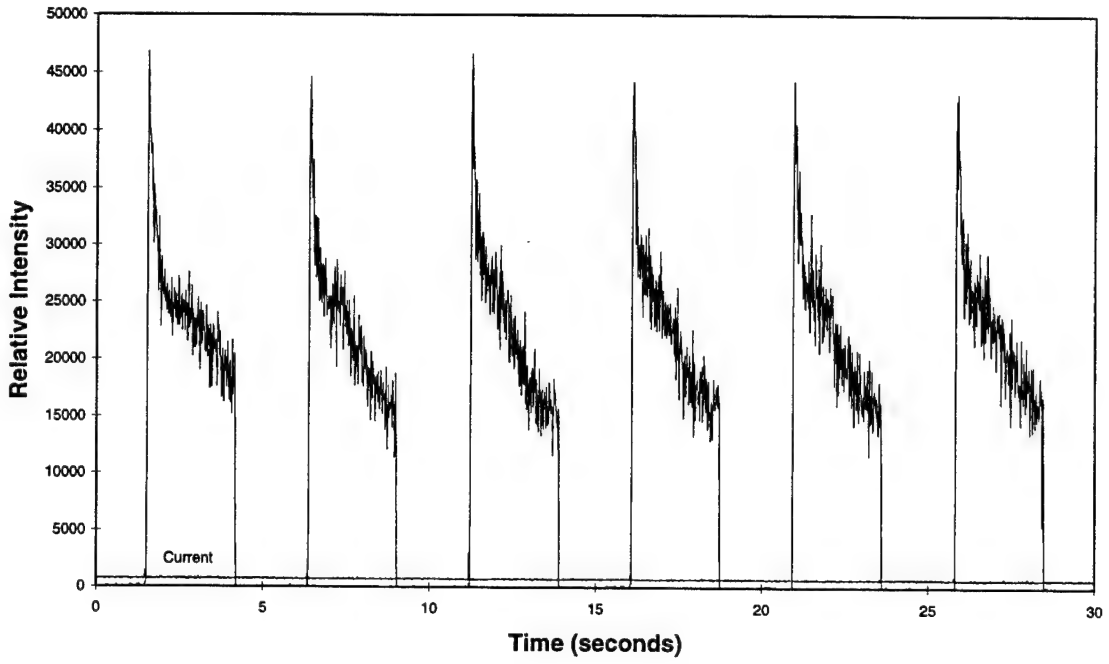

FIGURE 17: **THE SIX BOMBARDMENTS SUMMED TO YIELD FIGURE 16 (TOP CURVE)**

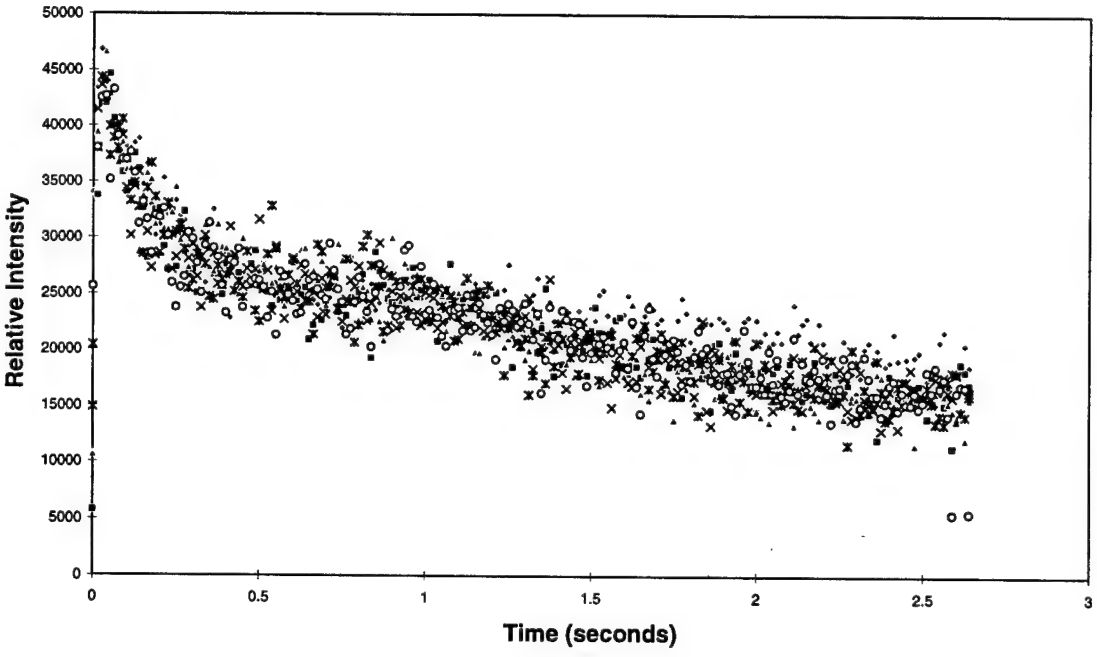

FIGURE 18: **THE SIX BOMBARDMENTS OF FIGURE 16 PLOTTED INDIVIDUALLY**

Table 3 suggests that the great differences that occur in the evolution of the aerogel are different at different wavelengths.

In a short term time dependent sequence (Figure 19) that was done directly before the higher emission 4500 Å sequence of Table 3 (*), the aerogel seems to be evolving over a short period of time (≤ 10 seconds).

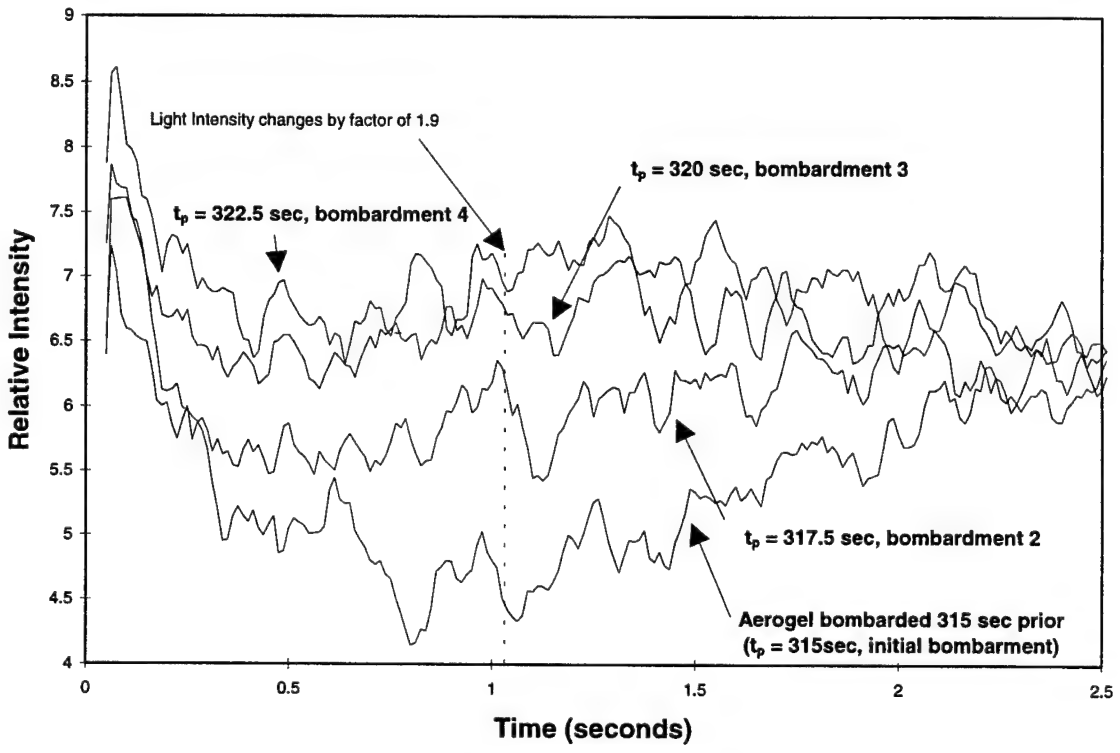

FIGURE 19: FOUR INDIVIDUAL BOMBARDMENTS OF A SHORT TERM TIME DEPENDENT SEQUENCE

λ4500 Å

i = 0.18 μA

T = 3.85 mm

Δt_p (from initial bombardment to bombardment 4) = 7.5 seconds

x = 0.50 mm

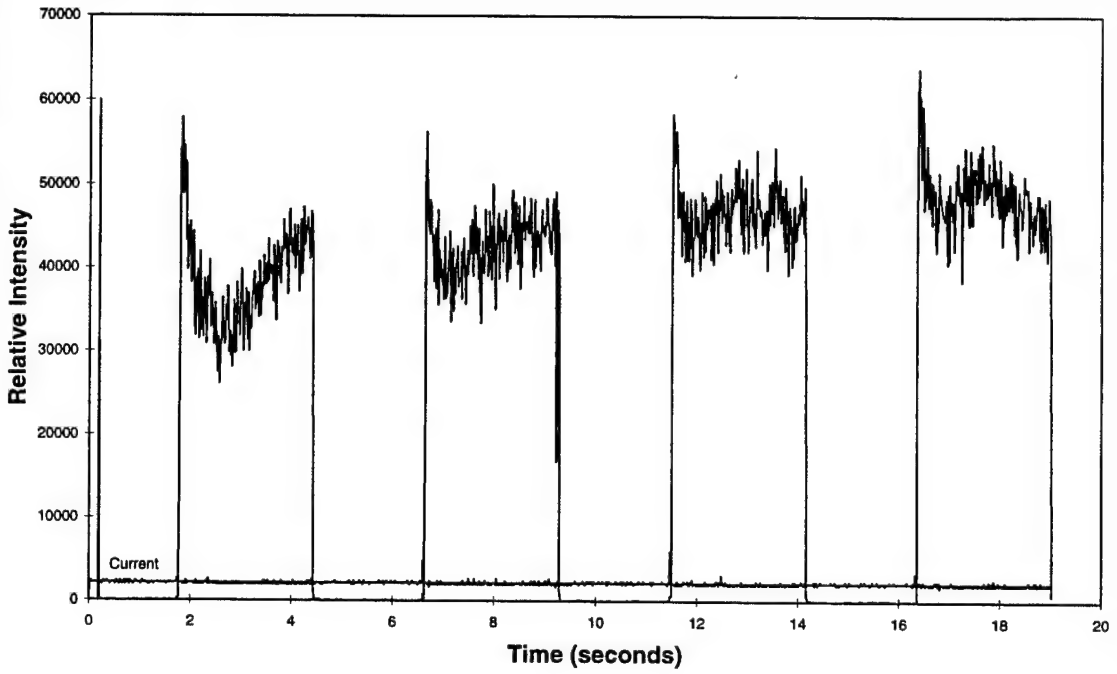

FIGURE 19B: THE FOUR INDIVIDUAL BOMBARDMENTS OF FIGURE 19 PLOTTED IN SUCCESSION (WITH CURRENT)

The aerogel had been bombarded for 315 seconds prior (t_p = 315 seconds) to this initial bombardment (bottom curve of Figure 19). Rather than adding these individual bombardments together, they are plotted individually to show how the aerogel intensity evolves. Figure 19b shows that the current is constant for the four individual bombardments. The change in emission that occurs in a time as short as 7.5 seconds is dramatic. The current is constant at 0.18 μA, yet at t = 1.025 seconds, the light intensity has changed by a factor of 1.9. This phenomenon was observed in another sequence shown in Figure 20. The bottom curve is from the first bombardment, the top curve is the sum of bombardments 3-12 (bombardment 4 not included--see Figure 20b). The aerogel

is 4.17 mm thick. The beam current is 0.32 μA. The wavelength scanned is 4500 Å . Figure 20b shows the current is constant. The fourth bombardment is omitted because of the random intensity variation that occurred in the middle of that scan.

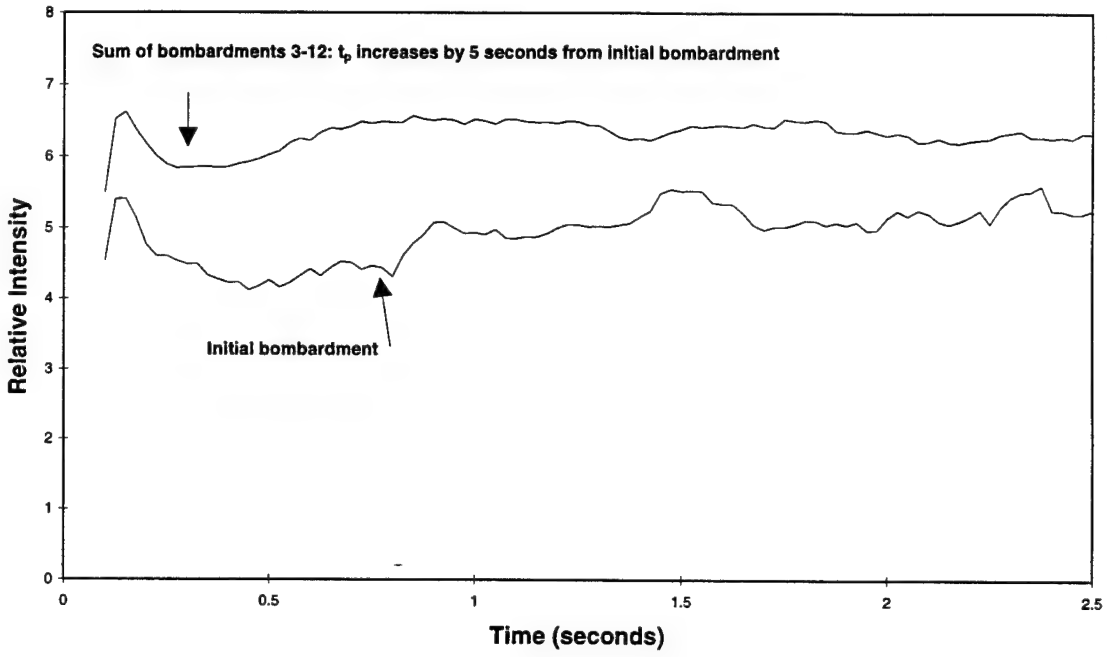

FIGURE 20: **FIRST BOMBARDMENT COMPARED TO THE SUM OF BOMBARDMENTS 3-12 (FOURTH BOMBARDMENT OMITTED IN SUM BECAUSE OF FLUCTUATION IN INTENSITY--SEE FIGURE 20B)**

λ4500 Å

i = 0.32 μA

T = 4.17 mm

Δt_p = 5 seconds

x = 0.50 mm

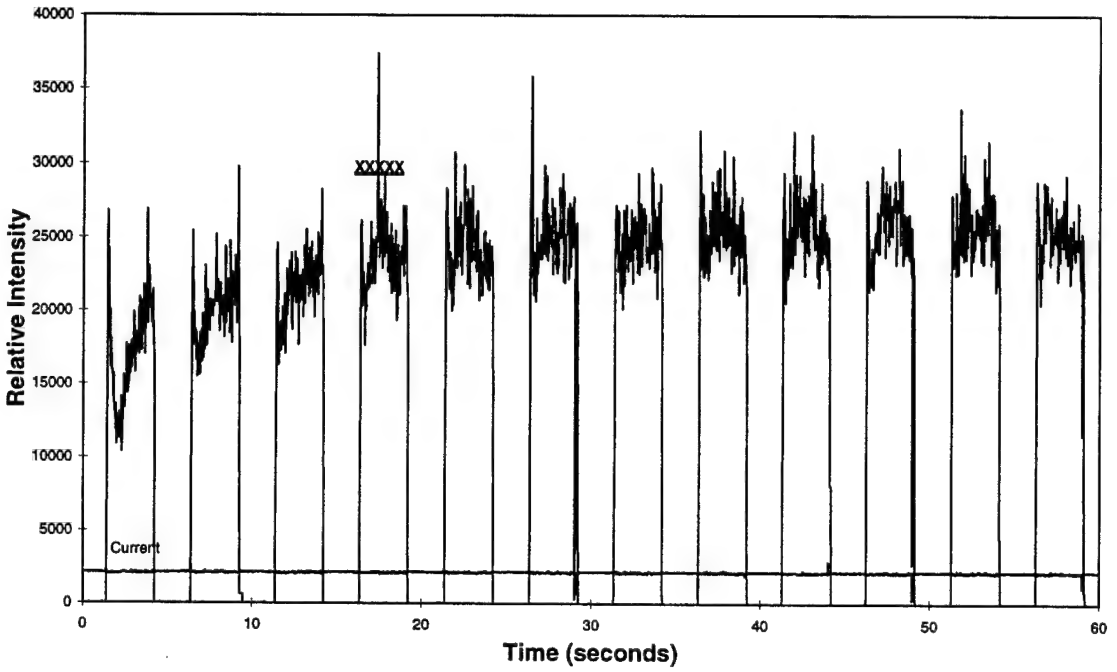

FIGURE 20B: THE 12 BOMBARDMENTS USED IN FIGURE 20 PLOTTED IN SUCCESSION (WITH CURRENT)

Another short term time dependent sequence is shown in Figure 21. It shows three individual plots: The initial bombardment, the second bombardment, and the sum of bombardments 3-12. Although Figure 21 does not exactly mimic Figures 19 and 20, it provides additional evidence that the aerogel is evolving in a short amount of time ($\leq$ 10 seconds) during bombardment. The aerogel is 4.17 mm thick. The beam current is 0.32 μA. The wavelength scanned is 5500 Å . Figure 21b shows the current is constant for each individual bombardment.

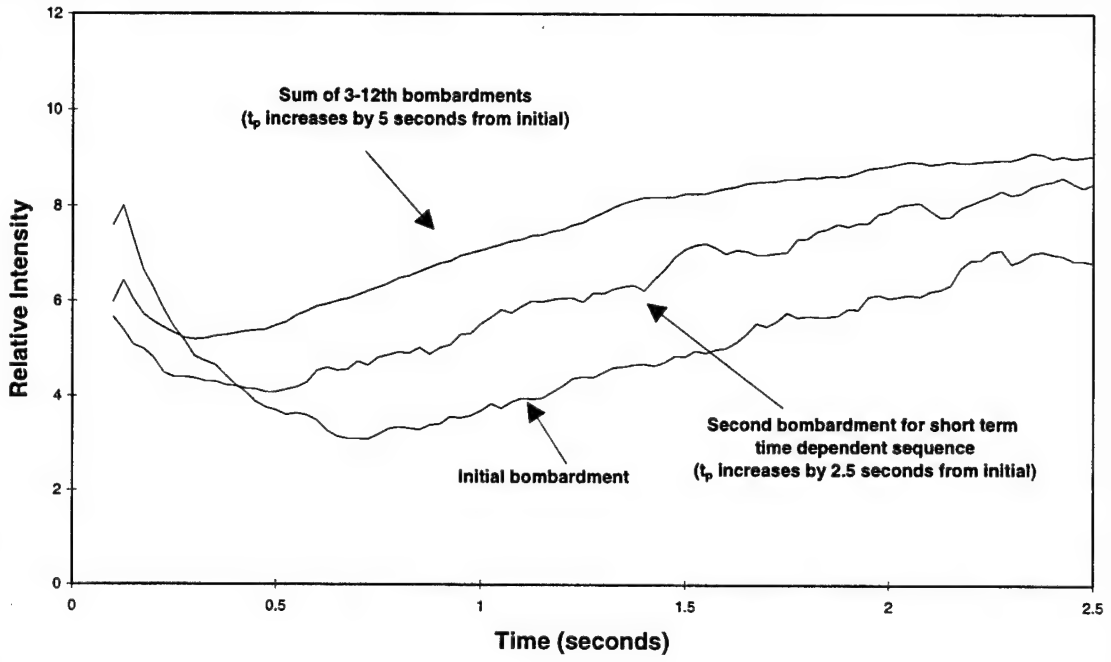

FIGURE 21: **THE FIRST AND SECOND BOMBARDMENTS, AND THE SUM OF BOMBARDMENTS 3-12**

λ5500 Å

i = 0.32 μA

T = 4.17 mm

Δt_p from initial bombardment = 2.5 seconds (middle curve), 5 seconds (top curve)

x = 0.50 mm

The curves in Figure 21 show not only how intensity can change over short bombardment periods, but also shows a change in shape. The intensity increases to above the initial peak by the end of the scan (2.5 seconds).

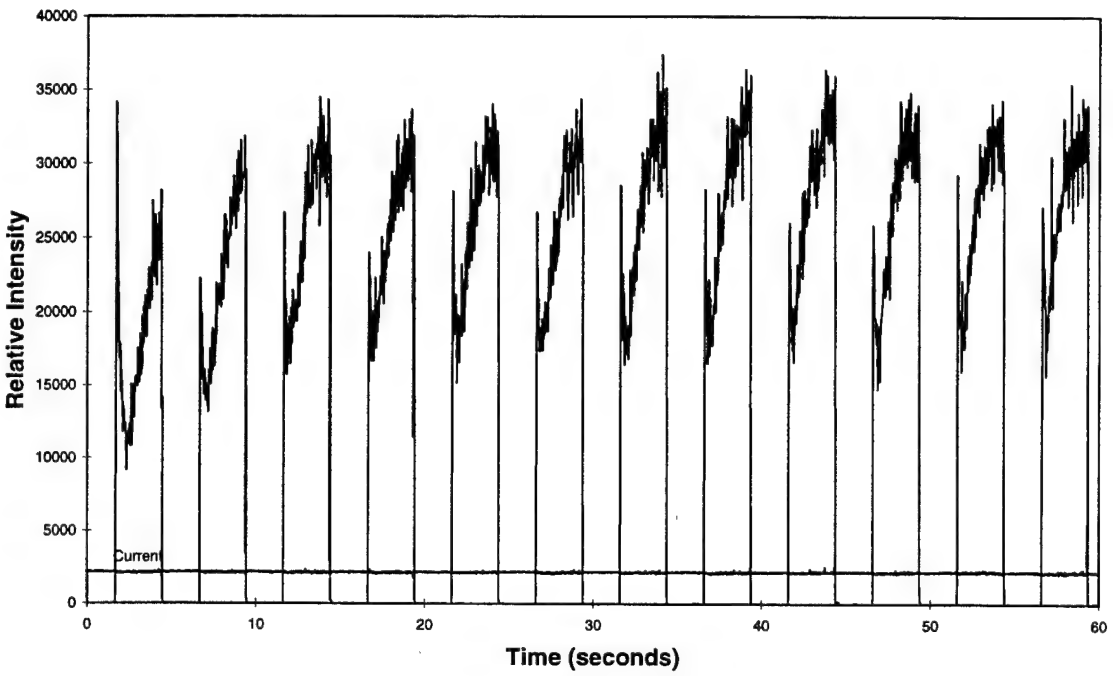

FIGURE 21B: THE 12 BOMBARDMENTS USED IN FIGURE 21 PLOTTED IN SUCCESSION

III. WAVELENGTH AND TIME BOMBARDED DEPENDENCE

In the previous short term time dependent sequences, the emission from the aerogel was erratic (Figures 19, 20, 21), whereas, often the time dependent emission is reproducible. Usually, the initial bombardment of an aerogel gives the highest intensity and the successive bombardments have intensities that are lower and fairly constant after the initial bombardment. This is shown in Figure 22.

The spectrum of the proton bombarded aerogel is of great interest. This information can be gained from spectral scans, but it is found that spectra (λ3500 - 7000 $\mathring{A}$) are continually distorted during the time the aerogel is bombarded during the scan (t_b) (see Section IV). Figure 22b shows the current is constant for the initial and second bombardments.

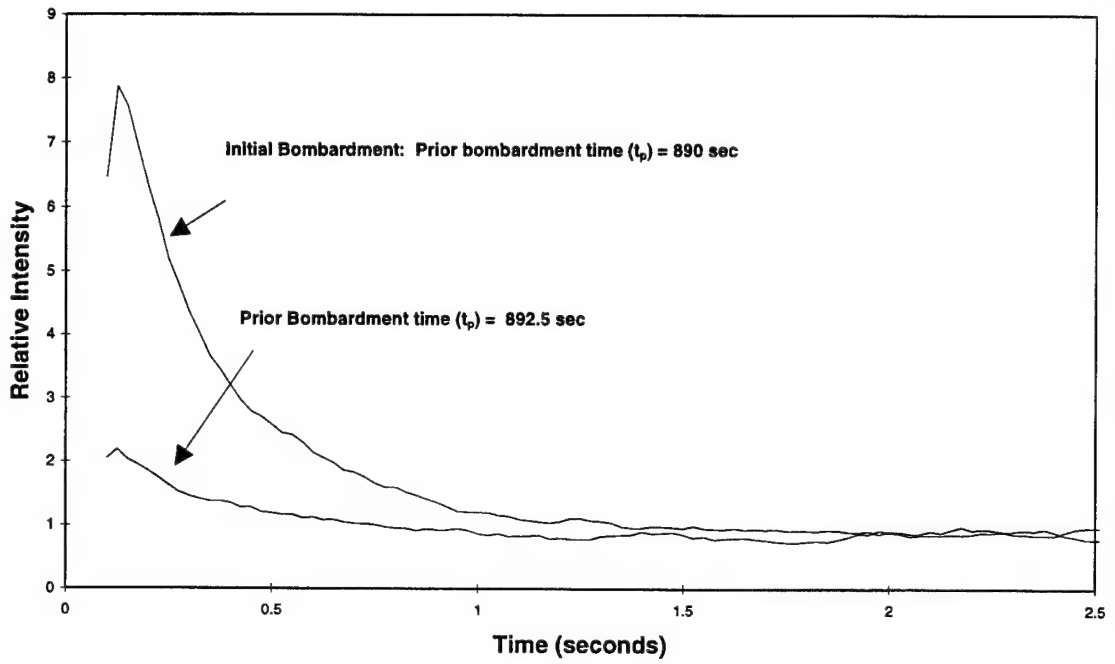

FIGURE 22: COMPARISON OF INITIAL TO SUCCESSIVE BOMBARDMENT

λ5000 Å

i = 0.32 μA

T = 4.17 mm

Δt_p = 2.5 seconds

x = 0.50 mm

The Scan in Figure 22 was taken at λ5000 Å . The trend of the initial bombardment emitting more light than successive bombardments is common at all wavelengths and usually occurs when the aerogel has been bombarded for times longer than 545 seconds. The initial bombardment emitting the most light occurred at all beam currents used. Table 4 shows how the light intensity dropped from the initial bombardment to the sum of the second through sixth bombardments for three aerogels of differing thickness (T) at three different currents (i). Time bombarded prior (t_p) is noted.

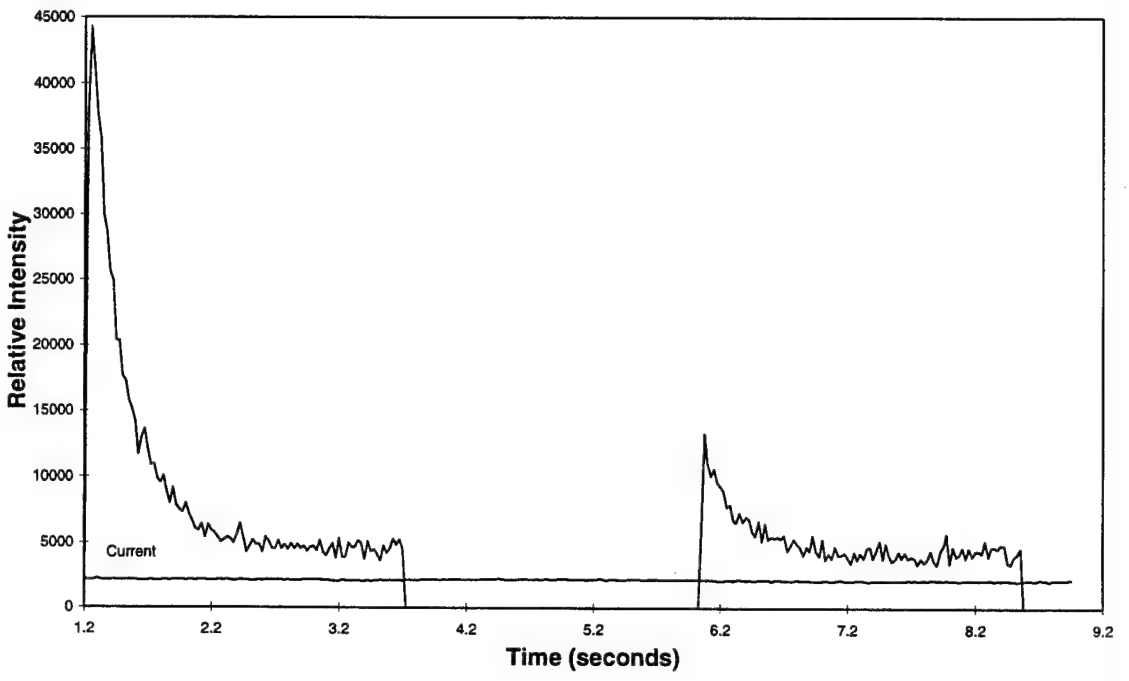

FIGURE 22B: THE TWO PLOTS OF FIGURE 22 PLOTTED IN SUCCESSION (WITH CURRENT)

Table 4: Comparison of Initial Bombardment to Successive Bombardments

Aerogel Thickness (mm)	Wavelength Observed (Angstroms)	Ratio Initial : 2^{nd}-6^{th}	Beam Current (μA)	t_p (seconds)
3.85	4000	1 : 0.55	0.18	580
	4500	1 : 0.51	0.18	650
	5000	1 : 0.58	0.18	685
4.17	4000	1 : 0.28	0.32	860
	4500	1 : 0.29	0.32	890
	5000	1 : 0.23	0.32	920
3.56	4000	1 : 0.51	0.14	710
	4500	1 : 0.51	0.14	740
	5000	1 : 0.44	0.14	770

It is also interesting to note that all of the initial bombardment intensities decayed to the same level as the second - sixth bombardments (top and bottom curves in Figure 22 end at the same intensity). The intensity for short term time dependent sequences in which the aerogel has been bombarded for less than 545 seconds tend to be erratic, like the short term evolution curves of Figure 19. They are very different from the reproducible scans recorded in Table 4.

IV. Time Dependence of a Spectrum

Aerogel spectra from λ3500 -7000 Å were examined for possible spectral lines (hydrogen). No lines have been found as of yet, however, other characteristics of the aerogel emission have been observed. The intensity maximum of aerogel spectra occurs in the range 4500 - 5300 Å , depending on the thickness of the aerogel and the beam current. In order to test the time dependence of an aerogel spectra at many different wavelengths, a spectrum was taken while intermittently opening and closing the beam flap. This showed how periodically halting the bombardment of the aerogel affected emission. This is shown in Figure 23.

Because the beam flap duty cycle was 1.2 (5.2 seconds on, 4.3 seconds off), the curve of Figure 23 has initial bursts of intensity each time the flap is opened while the spectrum is being taken. The scan rate was at 20 Å /sec so the duty cycle for this spectra can be converted to 52 Å on /43 Å off. Because the beam current is intermittently on and off of the aerogel during the scan, the location of the maximum of the spectrum cannot be

exactly determined, but it lies between 4250 and 4400 Å , much lower in wavelength than the location of the maxima of spectra recorded in Table 1 (and shown in Figure 24).

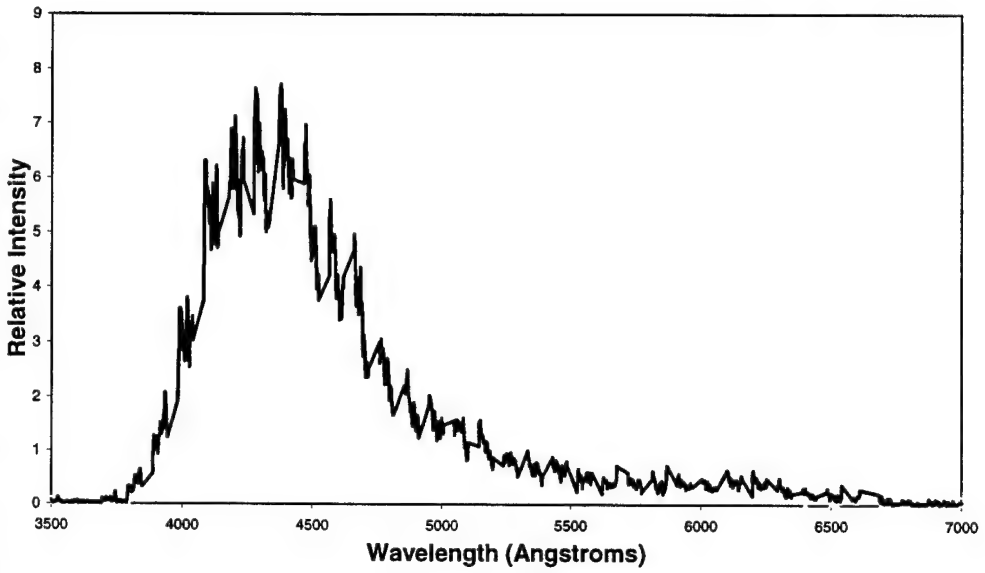

FIGURE 23: SPECTRUM FROM AN AEROGEL (λ3500 -7000 Å) USING A DUTY CYCLE

λ3500 - 7000

i = 0.12 μA

T = 5.50 mm

t_b = 98.5 seconds

x = 0.50 mm

Also, unlike spectra from aerogels that are bombarded continuously during a scan, the curve in Figure 23 dramatically drops in intensity at 5000 Å . The maximum of the spectrum in Figure 24 is 4 times larger than Figure 23 at 5000 Å . For comparison, Figure 24 shows a continuous bombardment (no duty cycle) spectrum from the same aerogel.

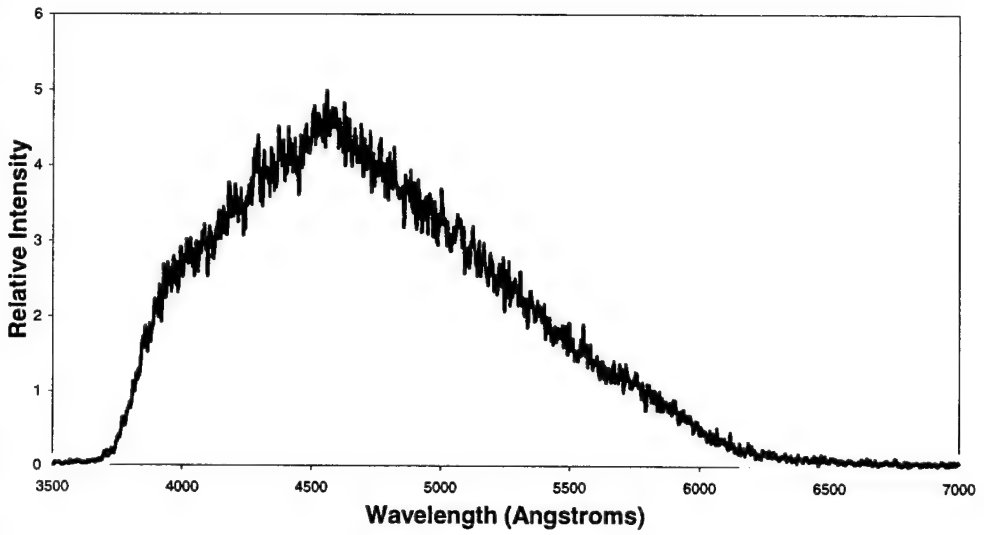

FIGURE 24: SPECTRUM FROM AN AEROGEL (λ3500 -7000 Å)--CONTINUOUS BOMBARDMENT

λ3500 - 7000

i = 0.12 μA

T = 5.50 mm

t_b = 180 seconds

x = 0.50 mm

V. CURRENT EFFECTS

Current effects on aerogel emission are very peculiar. As already shown in the first (Figures 15 and 15b) bombardment experiments, beam current fluctuations as small as 0.02 μA ($^{\delta i}/_{i}$ = 20 % for 0.1 μA, 7% for 0.3 μA) can cause a major change in light intensity. Changing the current by large amounts (≥ 0.2 μA) can cause an increase in emission intensity, and/or a change in the shape of a time dependent curve. Figure 25 shows the variations in intensities, shape, and decays of the initial bombardments on a

3.56 mm thick aerogel with two different currents. The higher current curve (top curve, 0.28 μA) has a peak that is 1.7 times larger than the lower current curve (bottom curve, 0.14 μA). Figure 26 shows the variations in the intensities of the sum of bombardments 2-5. In this case, the higher current curve has an intensity peak that is 3 times larger than the intensity of the lower current curve. Although both Figures 25 and 26 demonstrate that more light is emitted when the current is doubled, the amount is not a direct proportion. Figure 25 shows an intensity change of a factor of 1.7, Figure 26 shows a factor of 3. Non-linear current effects were common.

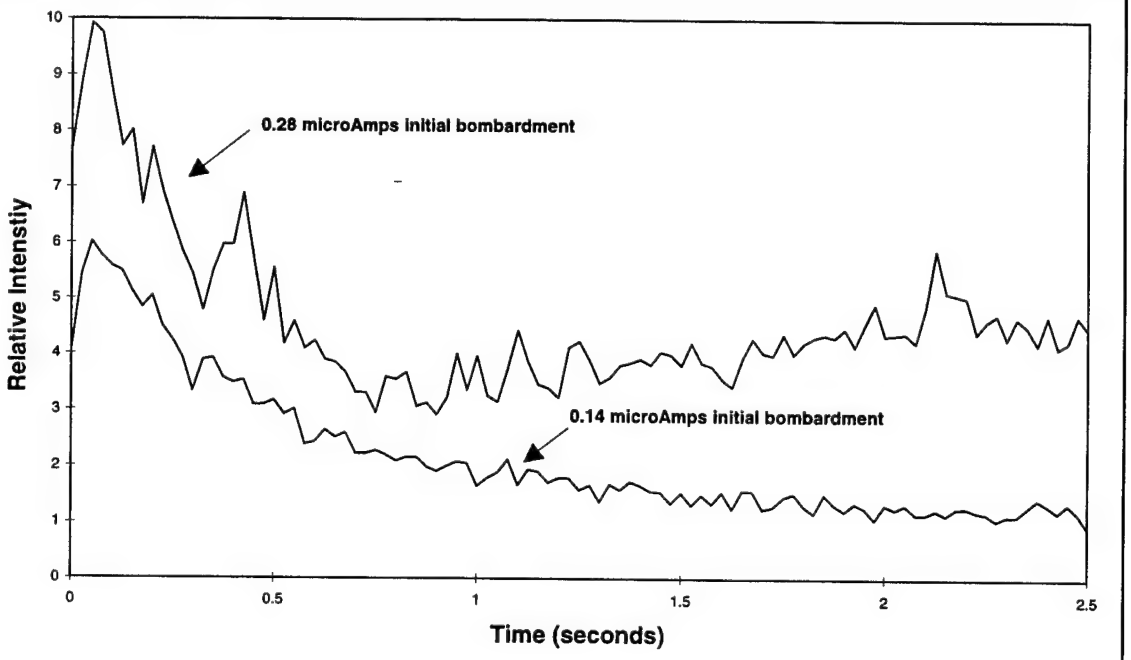

FIGURE 25: **THE LIGHT INTENSITY FROM THE INITIAL BOMBARDMENT ON AN AEROGEL AT TWO DIFFERENT CURRENTS**

λ5000 Å

T = 3.56 mm

x = 0.50 mm

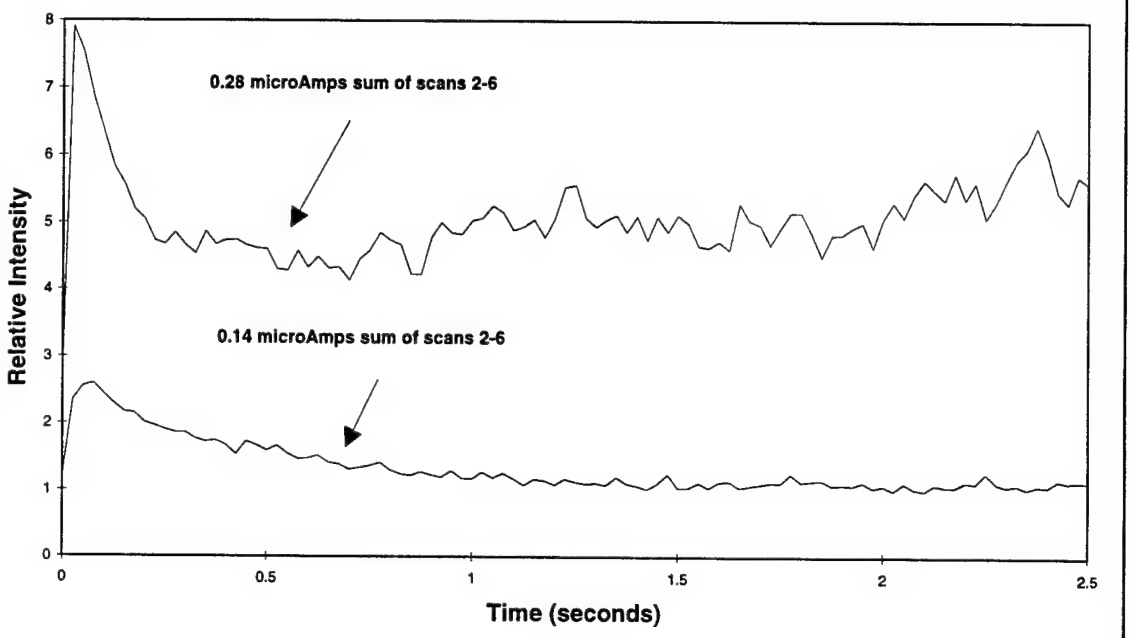

FIGURE 26: **THE LIGHT INTENSITY FROM THE SUM OF BOMBARDMENTS 2-5 ON AN AEROGEL AT TWO DIFFERENT CURRENTS**

λ5000 Å

T = 3.56 mm

x = 0.50 mm

The shape of time dependent emissions obtained at different currents also differ dramatically. The bottom curves of Figures 25 and 26 are smoother. The top curves are erratic and tend to rise after the drop from the initial peak--this was characteristic of data from higher current bombardment of aerogels.

VI. Observation Point (x)

Most emission intensities from gels decreased as the bombardment time increased (t_p) as shown in Figure 16. Whether the gels ability to react with the proton beam

decreases or whether the aerogel might be reacting more intensely farther into the aerogel (as x becomes greater) is a question of interest. In order to study this possibility, repeated long term time dependent scans were made, changing no variables except the observation point in the aerogel . Figure 27 is a the second bombardment of a 1.68 mm thick aerogel. The observation point is the front of the aerogel (x = 0.50 mm). The experimental conditions for the curve in Figure 28 are the same as in Figure 27, except that the observation point was moved 0.21 mm downstream from the front of the aerogel (x = 0.71 mm).

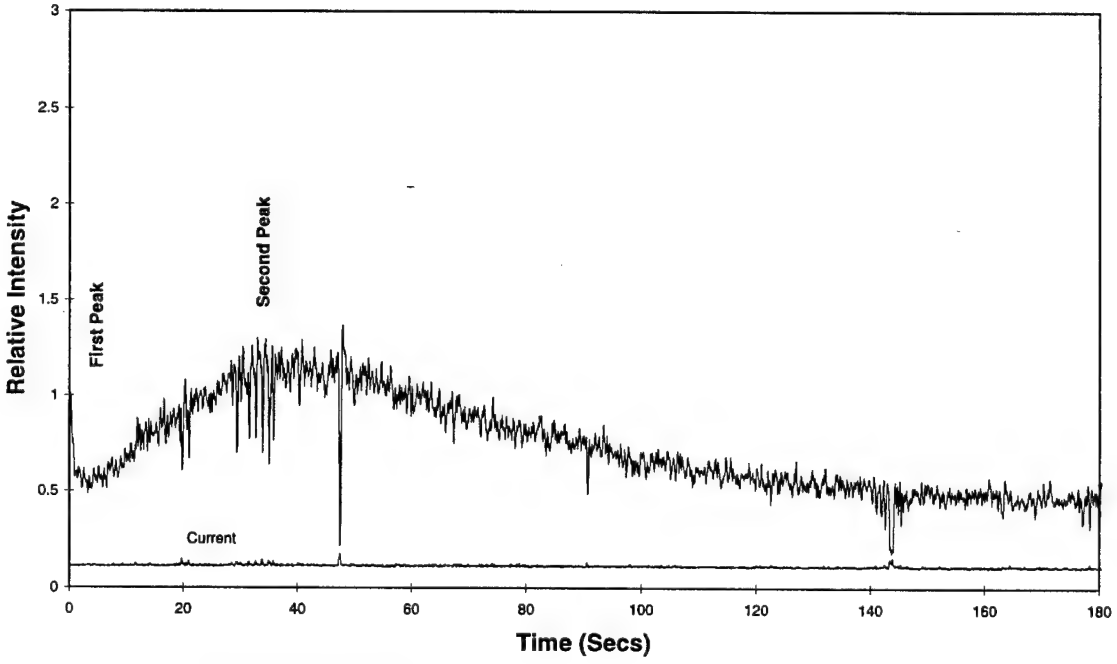

FIGURE 27: **THE SECOND TIME THIS AEROGEL HAD BEEN BOMBARDED (t_p = 180 seconds). LIGHT INTENSITY DECREASES TO A CONSTANT LONG TERM VALUE AT THE END OF THE SCAN.**

λ4000 Å

i = 0.12 μA

T = 1.68 mm

x = 0.50 mm

t_p = 180 seconds

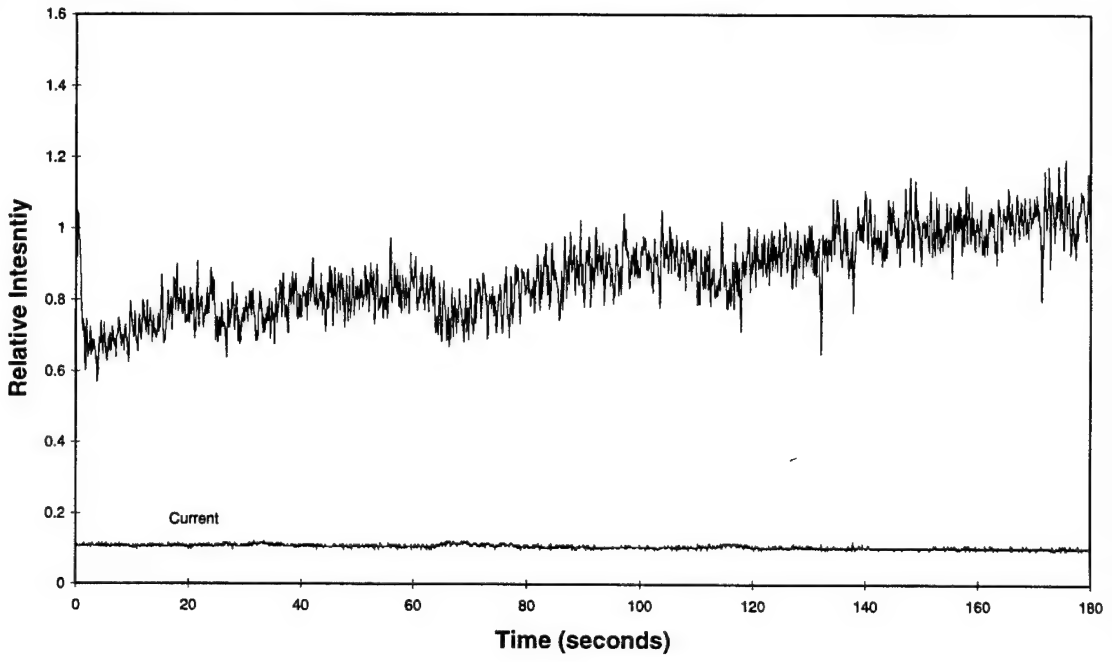

FIGURE 28: **SCAN TAKEN DIRECTLY AFTER THE SCAN SHOWN IN FIGURE 27. OBSERVATION POINT IS MOVED 0.21 MM DOWNSTREAM. INTENSITY IS INCREASING THROUGHOUT THE SCAN.**

λ4000 Å

i = 0.12 μA

T = 1.68 mm

x = 0.71 mm

t_p = 360 seconds

The experimental conditions for the curve in Figure 29 are identical to that of Figure 28 (x = 0.71 mm). The data for Figures 27, 28, and 29 were taken in succession.

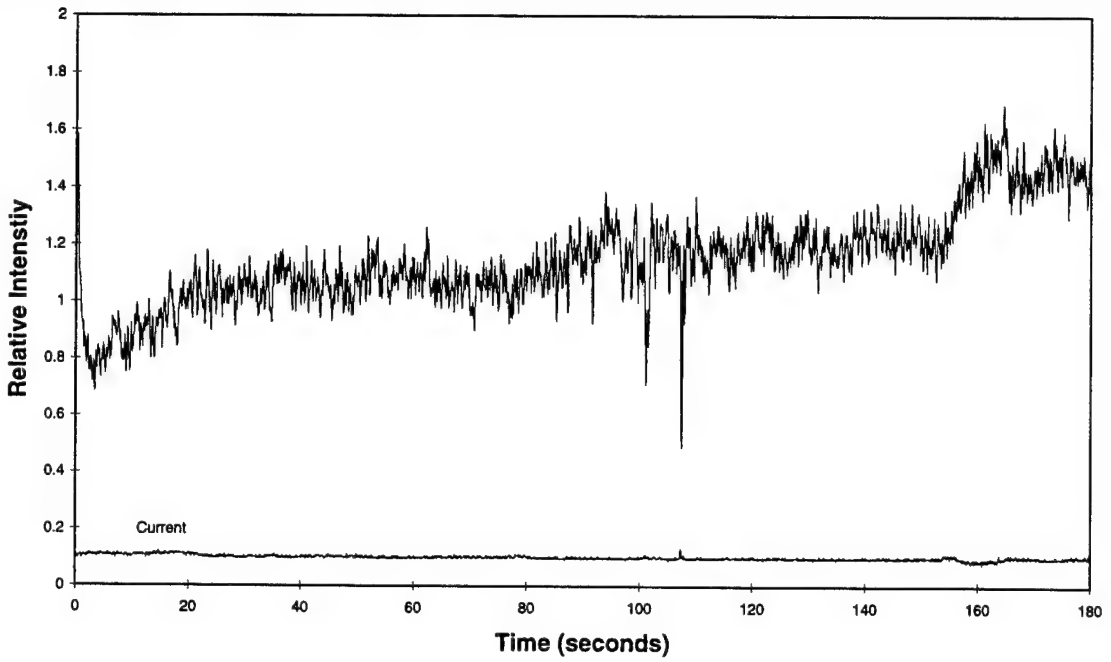

FIGURE 29: **SCAN TAKEN DIRECTLY AFTER THE SCAN SHOWN IN FIGURE 28. INTENSITY CONTINUES TO INCREASE THROUGHOUT THE SCAN**

λ4000 Å

i = 0.12 μA

T = 1.68 mm

x = 0.71 mm

t_D = 540 seconds

While the intensity usually decreases as one observes farther into the aerogel (see Figure 12) and the intensity decreases with increasing aerogel bombardment time, this is not the case for the Figures 27, 28, and 29. In these figures, the intensity increases as the observation point is moved downstream from the front of the aerogel, and, the intensity steadily increases as a function of time.

VII. THE DUTY CYCLE—CONTROLLING TIME SINCE LAST BOMBARDMENT OF THE AEROGEL

Figures 30 and 31 are two time-intensity curves taken with different duty cycles. They show that time since the aerogel was last bombarded (t_s) is of significant importance. The top curve of Figure 30 is the sum of 3 bombardments in which the duty cycle was 1/6 (5 seconds on, 30 seconds off). The bottom curve is the sum of 3 bombardments in which the duty cycle was 1/2 (5 seconds on, 10 seconds off). Aerogel thickness is 3.85 mm. Wavelength observed is $\lambda 4000\,\mathring{A}$. Beam Current is 0.17 μA.

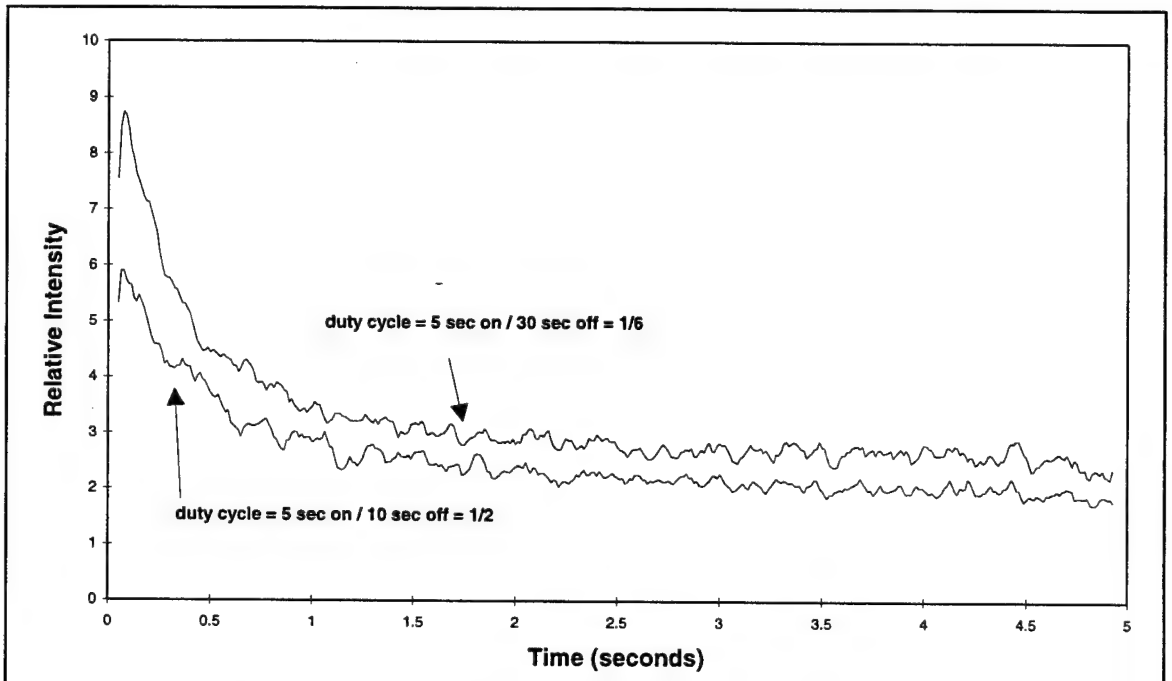

FIGURE 30: **TOP CURVE -- SUM OF 3 BOMBARDMENTS, DUTY CYCLE = 1/6**

BOTTOM CURVE -- SUM OF 3 BOMBARDMENTS, DUTY CYCLE = 1/2

$\lambda 4000\,\mathring{A}$

i = 0.17 μA

T = 3.85 mm

x = 0.50 mm

Δt_s = 20 seconds

Figure 31 is similar to 30, except in this case the top curve is the sum of 3 bombardments in which the duty cycle was 1/12 (10 seconds on, 2 minutes off). The bottom curve is the sum of 3 bombardments in which the duty cycle was 1 (10 seconds on, 10 seconds off). Aerogel thickness is 4.17 mm. Wavelength observed is λ4500 Å . Beam Current is 0.16 μA.

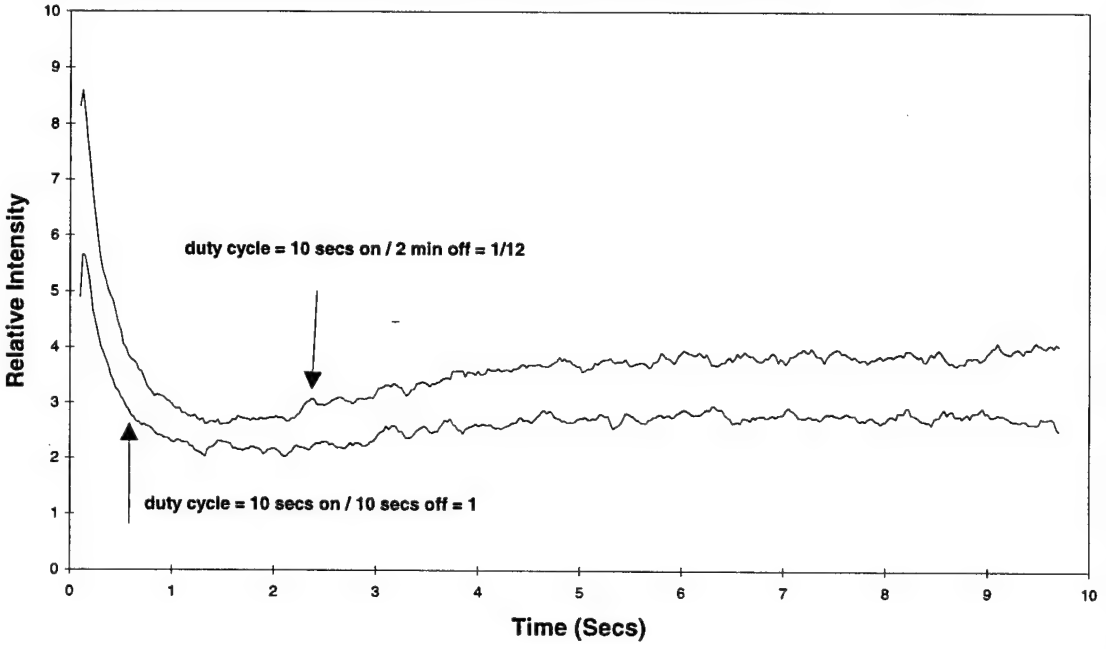

FIGURE 30: **TOP CURVE -- SUM OF 3 BOMBARDMENTS, DUTY CYCLE = 1/12**

BOTTOM CURVE -- SUM OF 3 BOMBARDMENTS, DUTY CYCLE = 1

λ4500 Å

i = 0.16 μA

T = 4.17 mm

x = 0.50 mm

Δt_s = 110 seconds

The duty cycle, and hence the time elapsed (t_s) since the aerogel has been bombarded, is directly related to its ability to emit light. The dependence of the emission on t_s is somewhat short term. Once (t_s) becomes greater than two minutes, it has little effect on emission.

VII. Long Term Time Dependence of an Aerogel

A long term time dependent scan of 30 minutes was taken from an aerogel with (t_p) of 22 minutes to see how long term exposure to the proton beam would affect its emission. The current was 0.19 μA. Figure 32 is a 30 minute scan (t_b = 30 min) on a 3.85 mm thick aerogel at 4500 Å . The scan in Figure 33a was taken under the same conditions as the scan in Figure 32, except bombardment was only 22.5 minutes (t_b = 22.5 min, t_p = 52 min). Figure 33b is the same scan as Figure 33a with a shorter time scale. Although the aerogel has been bombarded for 30 minutes longer for Figure 33a, it and Figure 32 are virtually identical. The scan for Figure 34a was taken under the same conditions as the two prior except bombardment was only 15 minutes (t_b = 15 min, t_p = 74.5 min) and current was 0.35 μA. Only the first 50 seconds of the scan is shown in Figure 34a. Figure 34b is the same scan as Figure 34a with the time scale extended to the full t_b = 15 minutes. Figure 34c is the current-time curve for the scan shown in Figure 34b. As one can see from comparing Figure 33b and 34a, the time decay is much longer for the higher current scan. Also, one can see the significant current dependence of emission from the aerogel by looking at Figures 34b and 34c. Usually, data with major

current fluctuations is not used, but it is a good example of how the aerogel emission decays as the current is intermittently bombarding the aerogel. The time between scans was four minutes (i.e. $t_s = 4$ minutes).

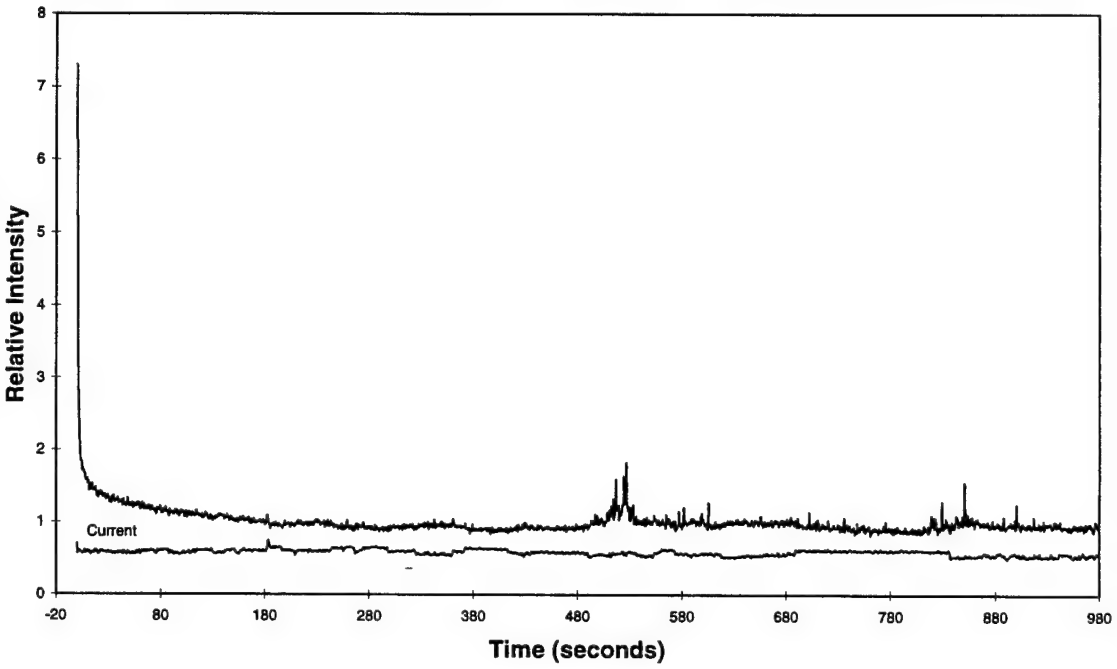

FIGURE 32: **LONG TERM TIME DEPENDENT SCAN OF AEROGEL, THE FIRST 16.3 MINUTES OF THE 30 MINUTE (980 SECOND) SCAN**

λ4500 Å

i = 0.19 μA

T = 3.85 mm

t_p = 22 minutes

t_b = 30 minutes

t_s = 4 minutes

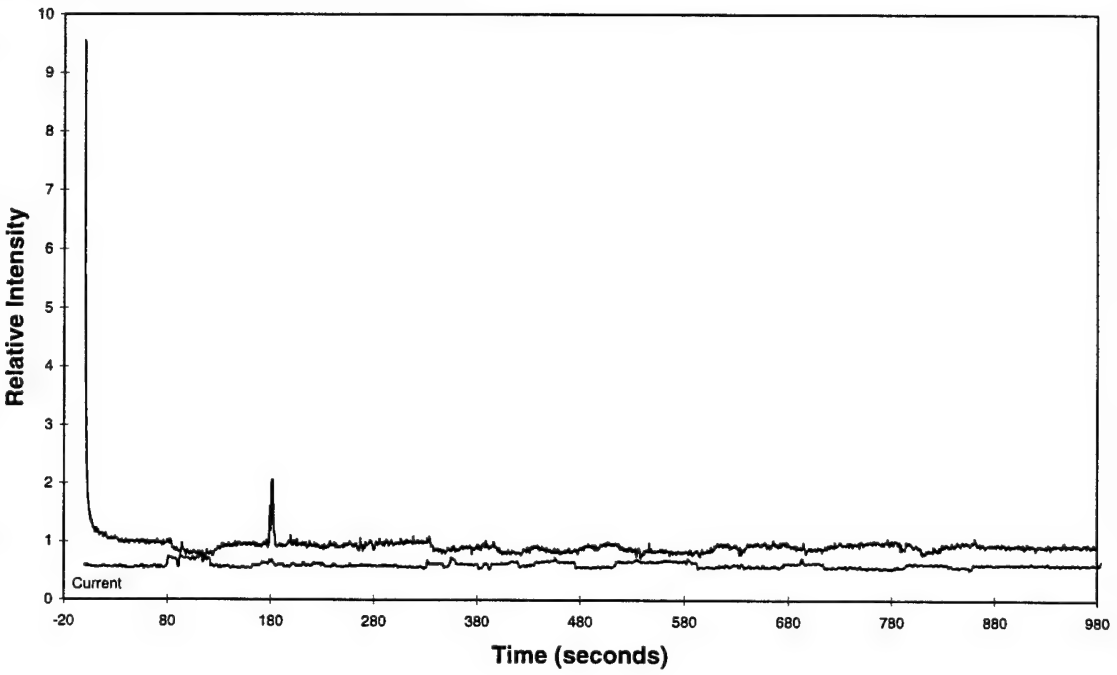

FIGURE 33: **LONG TERM TIME DEPENDENT SCAN OF AEROGEL, THE FIRST 16.3 MINUTES OF THE 22.5 MINUTE (980 SECOND) SCAN**

λ4500 Å

i = 0.19 μA

T = 3.85 mm

t_p = 52 minutes

t_b = 22.5 minutes

t_s = 4 minutes

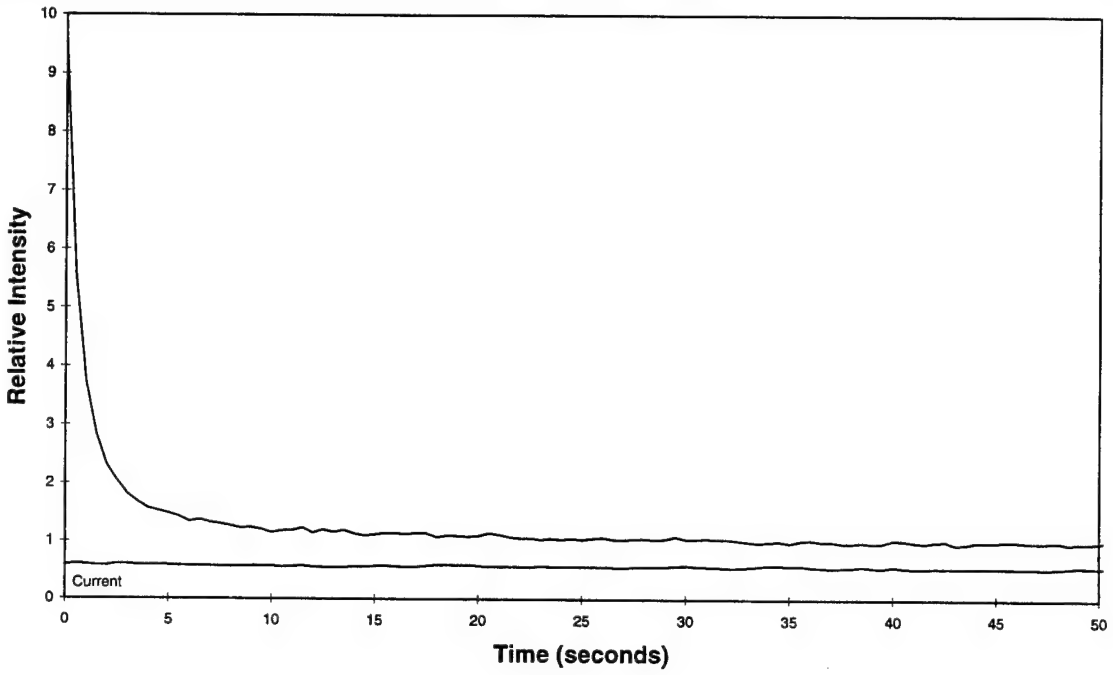

FIGURE 33B: LONG TERM TIME DEPENDENT SCAN (THE SAME SCAN AS IN FIGURE 33)--TIME SCALE IS DECREASED TO FIRST 50 SECONDS TO COMPARE DECAY TO FIGURE 34, i = 0.19 μA

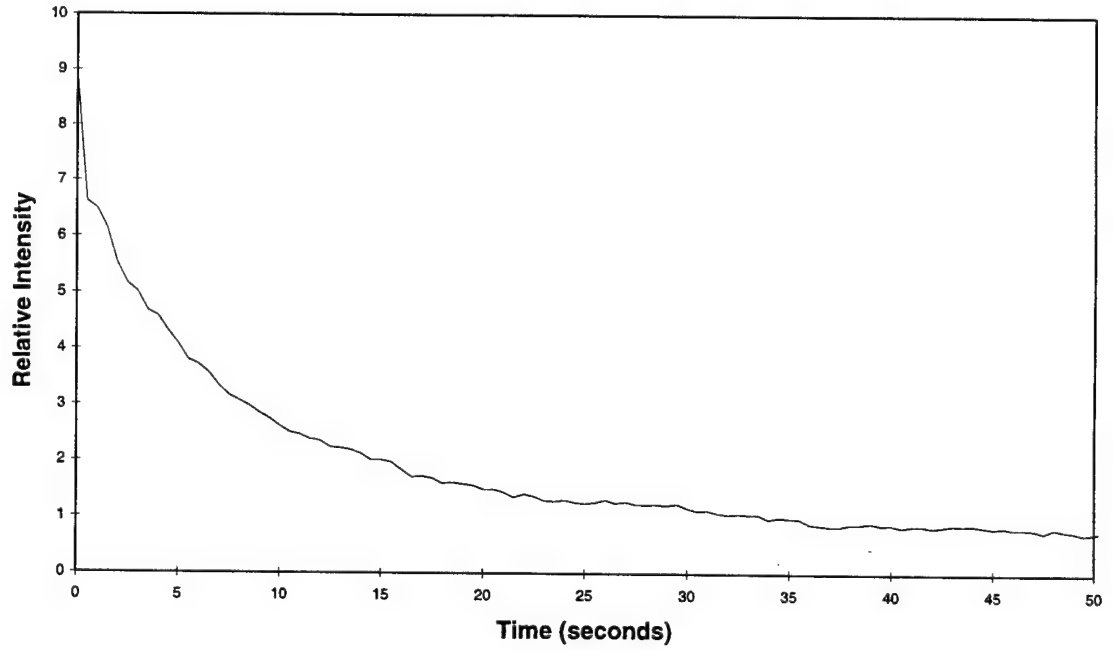

FIGURE 34A: THE FIRST 50 SECONDS OF A LONG TERM TIME DEPENDENT SCAN (FULL SCAN SHOWN IN FIGURE 34B). THE CONDITIONS ARE THE SAME AS THE SCAN IN FIGURE 33B EXCEPT THE CURRENT IS INCREASED TO i = 0.35 μA

λ4500 Å , i = 0.35 μA, T = 3.85 mm, t_p = 74.5 minutes, t_b = 15 minutes, t_s = 4 minutes

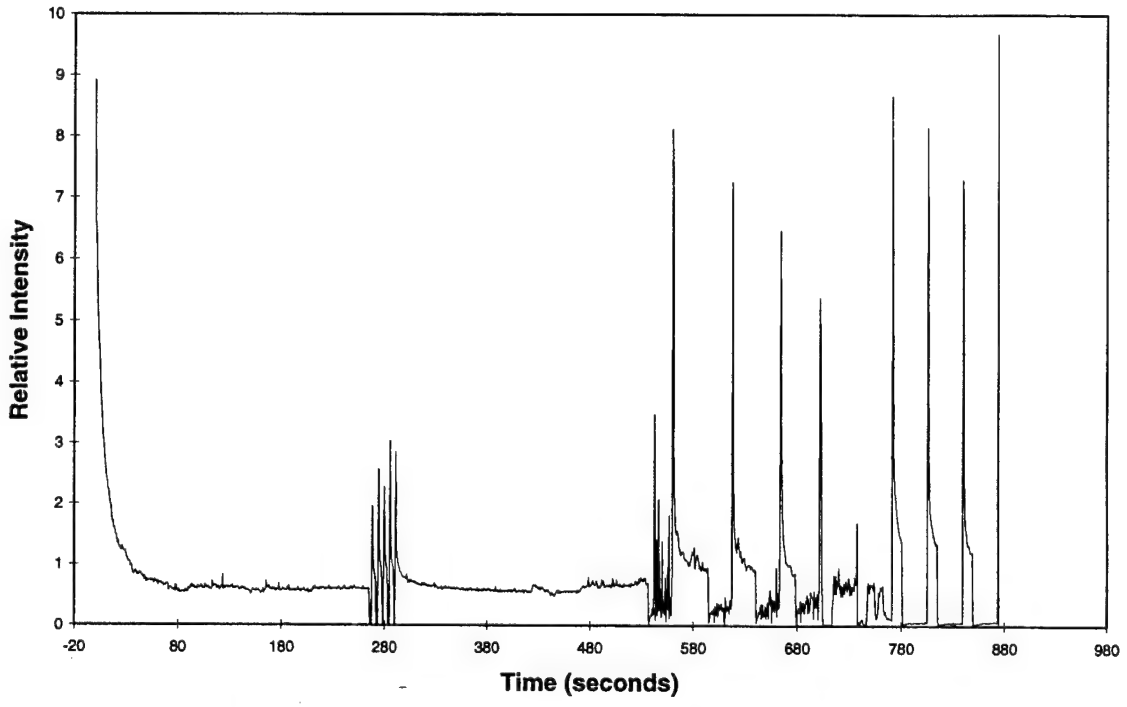

FIGURE 34B: LONG TERM TIME DEPENDENT SCAN OF 3.85 MM AEROGEL

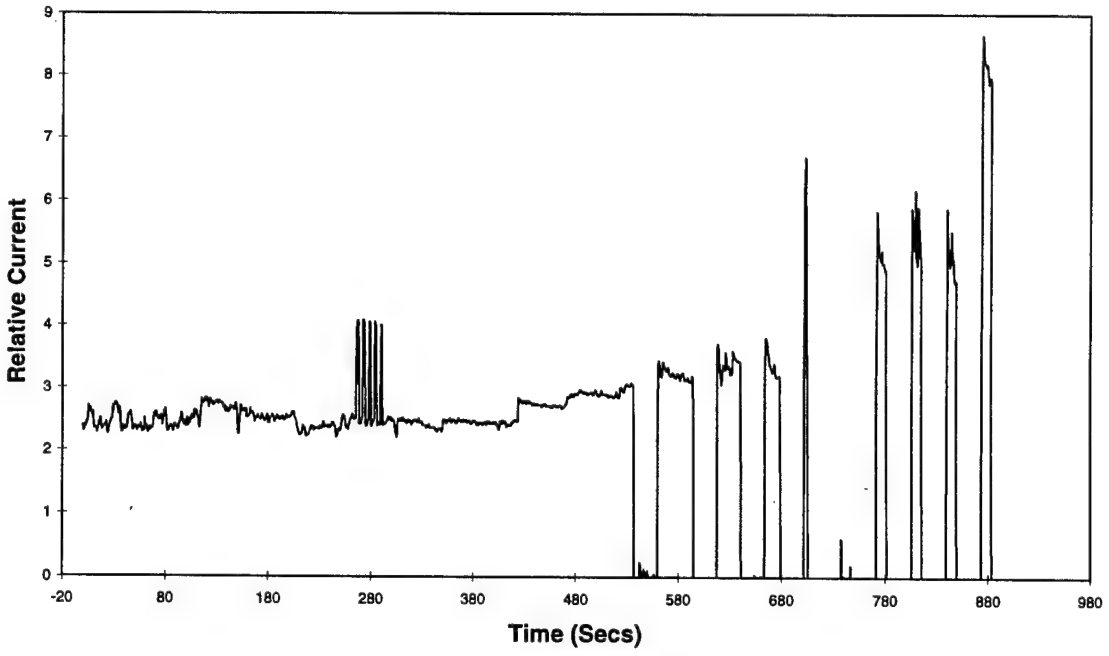

FIGURE 34C: RELATIVE CURRENT FOR SCAN SHOWN IN FIGURE 34B (i = 0.35 ± 0.03 μA for first 250 seconds)

Chapter 11: Discussion

I. The Spectral Emission from the Aerogel

Because aerogel emissions are dependent upon the slightest change in experimental parameters, a summary of some of the important results are given below.

1. Spectral Scans (λ3500 -7000 Å): Unlike previously thought, beam current, not just particle energy, has an affect on the shape of an aerogel spectrum (λ3500 - 7000 Å). Higher currents cause the spectrum to red shift. If bombardment of the aerogel is halted intermittently, the maxima of spectra are blue-shifted.
2. First Bombardment: The very first bombardment of an aerogel gives data very different than all other scans. The first bombardment produces an initial intensity peak when the beam first hits the aerogel, and then a higher peak between 30 and 45 seconds into the scan (λ4000 and 4500 Å).
3. Time Dependence: Three different time dependent parameters are important.
    a. (t_p)—time gel has been bombarded prior: This had significant effects on the intensity of light. The intensity can drop by a factor of 3.5 from a t_p difference of 105 seconds and grow by a factor of 1.9 in as little as 7.5 seconds.
    b. (t_s)—time since gel has been bombarded: Experiments showed t_s affects intensity. The longer the time interval between gel bombardment, the more intense its emission will be. After two minutes t_s, the affect is negligible.

c. (t_b)—time of bombardment for a data scan: Spectra from the same aerogel, one done with intermittent bombardment, the other with continuous bombardment, have different shape and maxima location.

4. Beam Current Effects: As seen in spectral and short term sequences, intensity increases with beam current, but not linearly. Also, in short term sequences, fluctuations in current as low as 0.02 μA ($^{\delta i}/_{i}$ = 20 % for 0.1 μA, 7% for 0.3 μA) caused major changes in light intensity. Short term sequences done with higher currents (i ≈ 0.30 μA) show curves become less smooth as current increases.

5. Evolution of an Aerogel: Time dependent scans taken from aerogels bombarded for less than approximately 550 seconds often show an erratic transformation of the gel within as little as 4 individual 2.5 second bombardments. The light intensity grows by a factor of 1.9. Scans taken after approximately 550 seconds of aerogel bombardment are more reproducible.

6. Observation Point: After the aerogel has been bombarded for approximately 6 minutes, an increase in intensity is seen when the observation position is moved farther downstream from the initial maximum emission point of a gel (the front). This indicates that the location of the maximum emission point (downstream from x = 0) changes with time.

II. Comparison to Beam-Foil and Beam-Gas Experiments

It is surprising that beam-aerogel experiments have produced no spectral lines. But, some similarities between other targets and aerogels were observed. Foils that had the same nominal thickness gave variations in light intensity from a proton beam as large as 20%. This was attributed to small amounts of surface contaminates (Bashkin, 1968). Some of these same problems might occur in aerogels. Gels could be slightly contaminated, not just on the surface, but inside of the porous material. Used foils emitted more light than new foils, whereas used aerogels emit less light than new ones. While foil experiments had a limited number of controllable variables, more variables seem to affect the emission of an aerogel. Good statistics are difficult to achieve because the time an aerogel has been bombarded is a significant variable. But, unlike beam-gas experiments, the target chamber is a vacuum. The point where the proton beam exits the aerogel ($x_e = T$) has not been established because no particles have been observed exiting the aerogel. The beam particles (protons) may be scattered out or stopped by the aerogel itself.

III. Scattering of Ions

The Rutherford scattering equation predicts the number of particles that will scatter through an angle θ for a foil (Thornton, 1993). This equation applied to a thin gel (1 mm) predicts the aerogel will scatter 85% of the bombarding ions through an angle of 1.5 degrees or more, but only 2% of the particles will scatter at an angle greater than 10

projected path length of a 1 MeV proton in a SiO_2 aerogel is 0.79 mm. Our observations uphold this calculation—no protons have been observed exiting the thinnest aerogel used in our experiments (1.68 mm). Thinner aerogels will be necessary in order to get a significant number of protons penetrating the entire aerogel thickness.

A rough calculation using the empirical formula derived from the Bethe equation is shown below. This calculation *does not* integrate over the change in energy from the proton's initial contact with the aerogel to it stopping inside of the aerogel.

For Oxygen

$\beta^2 = 0.002$ $A := .004079$ $a_j :=$

$E := 1000$ $B := 1.046\,10^4$

-6.734
3.019
-0.4748
.0371
-.0007669

For Silicon

$\beta^2 = 0.002$ $A := .007138$ $a_j :=$

$E := 1000$ $B := 6194$

-6.294
2.538
-0.3628
.0222
-.0004956

Empirical formula derived from the Bethe stopping power formula and experimental results[14].

[14] This is the formula for particle energies of 1 MeV and greater. The empirical formula for energies between 10 keV and 1 MeV confirms the calculations shown.

$$S_{O_1} := \frac{A}{\beta^2}\cdot\left[\left(\ln\left(\frac{\beta^2\cdot B}{1-\beta^2}\right)-\beta^2\right)-\sum_j a_j\cdot\ln(E)^j\right]$$

S_{O_1} = 2.217 High energy value in ev/10^{15} atoms/cm^2 (6)

for Oxygen

S_{Si_1} = 8.291 High energy value in ev/10^{15} atoms/cm^2

for Silicon

A, B and a_j's are all experimentally derived coefficients specific for each element

$\beta = v/c$

E = bombarding particle energy (KeV)

$E/d_O = So_1$ (eV - cm^2/10^{15} atoms) 0.2*10^{21} (O atoms/cm^3) = 0.44 KeV/μm for O_2

$E/d_{Si} = Ssi_1$ (eV - cm^2/10^{15} atoms) 0.1*10^{21} (Si atoms/cm^3) = 0.829 KeV/μm for Si

$$1/(E/d_O + E/d_{Si}) * E = 0.79 \text{ mm}$$

The projected path length of a proton through a 1 mm SiO_2 aerogel of density 0.1 grams/cm^3 is 0.79 mm. Because the rough calculation yielded a value on the same order of magnitude as the thickness of our aerogels, a computer program was used to integrate over the change in energy to get a more accurate answer. The computer calculation that integrates the Bethe equation over the change in energy yields a projected path length of

0.32 mm, still on the same order of magnitude as the thickness of our aerogels (Biersack, 1989).

V. Luminescence

Deceleration of ions by the aerogel could cause visible radiation in the form of luminescence. Luminescence is generally described as the process by which a material generates non thermal radiation that is characteristic of the particular material. In particular, if luminescence is the fundamental process for which radiation is being emitted from an aerogel it would specifically be called ionoluminescence. Most luminescence phenomena occur when the luminescing material is not in equilibrium within itself or with the its surroundings. A majority of absorbed excitation energy is transformed into luminescence radiation rather than into heat (and concurrent thermal radiation) or electron emission (Leverenz, 1968). Luminescence is excited by charged particles with energies ranging from 2 - 10^6 eV. Emitted photons are in the visible range. Luminescing materials are very sensitive to temperature. Above a critical temperature (a critical temperature for aerogel luminescence has not yet been established), luminescence efficiency decreases rapidly to vanishingly low values (Leverenz, 1968). In the luminescence excitation process, ions usually give up their energy in the from of successive inelastic collisions with free or bound electrons (in this case, electrons of the SiO_2 molecules).

Also, the coating on the front of the aerogel from bombardment or contaminates inside of the gel (lodged protons) could be affecting its luminescing efficiency. Leverenz

says the additionally impurity incorporated in a luminescing material when the absorbed primary ion remains, at least temporarily, greatly reduces the luminescence efficiency (1968).

VI. Thermal Effects

No temperature measurements were made on aerogels during the experiments, so it is difficult to assess thermal affects. A few preliminary calculations are discussed here.

The thermal conductivity of an aerogel is 0.007 milliwatts/m-K. Knowing this, a temperature gradient from the front to the back of the aerogel can be determined (Serway, 1990). If it is assumed that all the of the energy going into the aerogel was converted into heat, the temperature would drop at a rate of 143 K/μm from the front to the back of the aerogel. If the aerogel is modeled as a silica brick and is assumed to reach thermal equilibrium as it is bombarded, the temperature of the aerogel would be 324 K (CRC Handbook, 1975-76; Serway, 1990). The combination of those two calculations indicates that temperature increase would occur at the front of the aerogel and drop to the temperature of its surroundings (room temperature) within the first few microns of the aerogel. Oddly enough, the distance for the temperature to drop to that of its surroundings is the same distance over which the bombarding protons are stopped.

The specific heat of an aerogel is not known, but if it is assumed to be as good as that of water, which has the highest specific heat of common earth materials, the temperature change from it and the air surrounding it would be 2.4 K after 1 sec of bombardment, 24 K after 10 sec of bombardment, and 430 K after 3 min of bombardment

(Serway, 1990). If it is assumed the aerogel has a specific heat closer to glass, the temperature change could reach 120 K in 10 seconds. This indicates that the aerogel could be heating up for long term time scans, but also makes the assumption that all of the energy goes into heating the aerogel.

Because we know that all the energy entering the aerogel is not converted into internal thermal energy (after all, we see visible radiation) and we don't know how long it takes the gel to reach thermal equilibrium (assuming it does), calculations predicting aerogel temperatures of 324 K (51 C°, 124 F°) only give of us an idea of what thermal effects might be occurring. These calculations are shown in Appendix C.

Chapter 12: Conclusions

The aerogel is a unique and interesting solid, in that it can have extremely low densities and up to 99.5% porosity. It has incredible insulating capabilities and has no constant crystal structure. These unique properties evidently affect aerogel emission. We detected no protons transmitting through the aerogel. Theoretical calculations show that protons will not propagate the entire thickness of the aerogel unless it is thinner than about 0.3 mm.

Scattering calculations reveal that 85% of the particles would scatter at an angle of 1.5 degrees or more (only 2% will scatter at angles greater than 10 degrees). This rough calculation assumes: 1) All nuclei are exposed to the bombarding particle and 2) the bombarding velocity is constant through the aerogel. Neither are true. Not all the nuclei will be affecting the bombarding particles at particular points in the gel since some nuclei

will be hidden behind others. Also, the bombarding particle is decelerating as it proceeds through the aerogel. Rutherford scattering is directly proportional to the number of nuclei affecting the bombarding particle and inversely proportional to the velocity of the bombarding particle. These two variables are not constant and must be taken into consideration. Bethe's equation predicts that the protons are stopped within the first 0.3 mm of the aerogel thickness. This indicates that the protons most likely stop inside of the aerogel before they scatter out. Because they are decelerating (losing energy) so fast, the Rutherford scattering effect will increase dramatically, but in order for protons to Rutherford scatter out of the aerogel, the protons would have to be scattered at angles greater than 100 degrees just as they make contact with the aerogel. If they penetrated the aerogel farther than 0.1 mm, it would be impossible for them to escape because our aerogel thicknesses are larger than 1.68 mm, the face of our aerogels are approximately 100 mm^2 (i.e. 10 mm height and width) and a 1 MeV proton will stop within 0.32 mm. Knowing this, we assume that the protons decelerate to 3/4 their initial energy at 0.1 mm inside the aerogel. At 3/4 their initial energy, only 1/27000 protons would scatter at an angle greater than 100 degrees (assuming no more deceleration). These would be the only protons capable of scattering out of the aerogel, but even those (1/27000) protons are unlikely to scatter because they would experience deceleration on the way back out of the front of the aerogel. Rutherford Scattering is predicted to be insignificant.

Luminescence is the most likely radiation source of the aerogel. Proton bombardment may cause a non-equilibrium of charge in the aerogel that is transformed into radiation in the form of luminescence. If protons at a current of 0.1 μA were

propagating through a 1 mm gel, only 37 protons would be in the gel at one time, not nearly enough to affect the equilibrium of the 10^{21} SiO_2 molecules in the aerogel. Assuming all the protons stop in the aerogel (a good assumption considering the Bethe equation calculations), 10^{11} protons would be inside of the aerogel after one second[15], 10^{-9} of the number of SiO_2 molecules in the aerogel—still an incomparable amount compared to the 10^{21} SiO_2 molecules, but a significant number of positive charges nonetheless. Even if the protons cause relatively no change in the equilibrium of the aerogel, the physical mechanism for light emitted from an aerogel is most likely protons giving up energy in the form of inelastic electron collisions which causes luminescence. The stopping power of the medium (the aerogel), which was calculated using the empirical form of the Bethe equation, is based on electron collisions.

The strict temperature dependence of luminescence could be an explanation for the time dependent peaks observed. If the protons are increasing the temperature of the aerogel, the initial peaks could decay as luminescing efficiency decreases. Since impurities caused by lodged ions cause luminescing materials to loose efficiency, both the possibility of protons lodged in the aerogel and the coating on the front of the gel could be responsible for some of the degradation of emission intensity from the aerogel over time.

No temperature measurements were done, but calculations predict the aerogel temperatures could be 324 K or higher. If the luminescing aerogel degrades in intensity because of the temperature dependence of luminescence, thermal radiation could be the

[15] It would take 32 years of bombarding the aerogel with protons at a current of 0.1 μA to get the number of protons inside of the aerogel on the same order as the number of SiO_2 molecules.

source of some of the visible radiation from the gel. A gel spectra (λ3500 -7000 $\mathring{A}$) blue shifts for spectrum scans made with a duty cycle. The thermal radiation may be mostly infrared for the spectrum made with a duty cycle, whereas, for a constantly bombarded aerogel, the thermal radiation may increase enough to be seen in the redder part of the spectrum. Temperature measurements will answer questions regarding thermal effects.

The properties of the aerogel are quite important. Non-uniformity of aerogels could cause many of the erratic observations seen. Now, aerogels can be cut with more precision than ever, enabling the production of aerogels of identical thickness for future experiments. These aerogels should produce more consistent and reproducible results.

Chapter 13: Further Suggestions

The following are some suggested improvements to spectroscopic aerogel experiments.

1. Move the faraday cup closer to the aerogel to measure scattering and penetrating beam particles. This will become more important as thinner aerogels and higher beam energies are used.
2. Use the new saw mechanism created to cut aerogels more precisely to cut aerogels to thicknesses less than or equal to the projected path length of a 1 MeV proton through the SiO_2 aerogel. The energy of a bombarding proton should be increased to increase its projected path length. Lower or higher density gels should be purchased or made to change the stopping power of the aerogel. With a thinner aerogel, higher particle energy, and lower density aerogel, full proton penetration through the aerogel will occur.

3. Use back light calibration to measure the thickness of all aerogels so the experimenter will not have to risk ruining an aerogel specimen with calipers.
4. Study the aerogel itself. It could be recycled in the target chamber from low to high pressure to understand the importance of residual gas or charging.
5. Install a temperature probe to measure the aerogel temperature during proton bombardment. Study thermal effects. Since temperature varies considerably throughout the aerogel, placement of the probe is important.

Appendix A

Procedure: To measures the time the flap took to open and close, a small laser light was centered on the middle of the tantalum flap. The flap speed was measured with different currents applied to the solenoid. An oscilloscope was used to measure the time for the flap to open and close.

Table 1: Time for Flap to Open as a Function of Current

CURRENT (amperes)	TIME TO OPEN BEAM (milliseconds)
.9	2
	1.5
	1.5
1	1
	1.25
1.1	0.75
	0.85
	0.75
1.2	0.6
	0.7
	0.75
1.4	0.55
	0.6

As one can see from the table, the time to open the beam up is dependent on the current. The time for the flap to close the beam off was constant at 2 milliseconds. The time to close the beam was not dependent on the current, it is only dependent on the recoil strength of the spring in the solenoid. During experiments, 1 ampere was used to power the solenoid.

Appendix B

Output of Computer Program: TRIM

The Path Length was calculated using 1 MeV Protons as the bombarding ion, SiO_2 with density 0.1 grams / cm^3 as the target.

```
                    (C) 1989 by J.P. Biersack and J.F. Ziegler
      ==> Version - 5.4 <==
Ion = H ( Mass = 1 )
Target = Si( 33 % ) + O( 67 % )
Density = 1.0000E-01 g/cm3
Disk File Name = HGEL
Stopping Units = keV / micron
```

Ion Energy	dE/dx Elec.	dE/dx Nuclear	Projected Range	Longitudinal Straggling	Lateral Straggling
100.00 keV	5.887E+00	9.449E-03	20.06 um	2.15 um	3.94 um
110.00 keV	5.844E+00	8.764E-03	21.73 um	2.20 um	4.08 um
120.00 keV	5.781E+00	8.180E-03	23.42 um	2.25 um	4.21 um
130.00 keV	5.703E+00	7.674E-03	25.13 um	2.30 um	4.34 um
140.00 keV	5.615E+00	7.232E-03	26.87 um	2.35 um	4.47 um
150.00 keV	5.520E+00	6.843E-03	28.64 um	2.39 um	4.60 um
160.00 keV	5.421E+00	6.496E-03	30.44 um	2.44 um	4.73 um
170.00 keV	5.319E+00	6.186E-03	32.28 um	2.49 um	4.86 um
180.00 keV	5.216E+00	5.906E-03	34.16 um	2.53 um	4.98 um
200.00 keV	5.013E+00	5.421E-03	38.02 um	2.65 um	5.24 um
220.00 keV	4.815E+00	5.015E-03	42.05 um	2.78 um	5.50 um
240.00 keV	4.627E+00	4.670E-03	46.25 um	2.91 um	5.77 um
260.00 keV	4.450E+00	4.373E-03	50.61 um	3.03 um	6.05 um
280.00 keV	4.285E+00	4.113E-03	55.15 um	3.17 um	6.33 um
300.00 keV	4.130E+00	3.885E-03	59.86 um	3.30 um	6.63 um
330.00 keV	3.918E+00	3.590E-03	67.26 um	3.57 um	7.08 um
360.00 keV	3.728E+00	3.339E-03	75.05 um	3.84 um	7.56 um
400.00 keV	3.504E+00	3.058E-03	86.04 um	4.28 um	8.24 um
450.00 keV	3.264E+00	2.771E-03	100.73 um	4.92 um	9.13 um
500.00 keV	3.060E+00	2.536E-03	116.44 um	5.58 um	10.09 um
550.00 keV	2.885E+00	2.340E-03	133.17 um	6.24 um	11.10 um
600.00 keV	2.733E+00	2.174E-03	150.87 um	6.91 um	12.17 um
650.00 keV	2.600E+00	2.032E-03	169.51 um	7.58 um	13.30 um
700.00 keV	2.482E+00	1.908E-03	189.09 um	8.27 um	14.48 um
800.00 keV	2.282E+00	1.703E-03	230.88 um	10.53 um	16.99 um
900.00 keV	2.118E+00	1.540E-03	276.14 um	12.69 um	19.69 um
1.00 MeV	1.980E+00	1.407E-03	324.72 um	14.82 um	22.57 um
1.10 MeV	1.863E+00	1.296E-03	376.54 um	16.93 um	25.62 um
1.20 MeV	1.761E+00	1.203E-03	431.49 um	19.05 um	28.83 um
1.30 MeV	1.672E+00	1.123E-03	489.50 um	21.18 um	32.20 um
1.40 MeV	1.592E+00	1.053E-03	550.53 um	23.33 um	35.72 um
1.50 MeV	1.521E+00	9.919E-04	614.50 um	25.50 um	39.39 um
1.60 MeV	1.457E+00	9.380E-04	681.37 um	27.70 um	43.20 um
1.70 MeV	1.399E+00	8.899E-04	751.10 um	29.93 um	47.16 um
1.80 MeV	1.346E+00	8.468E-04	823.66 um	32.18 um	51.25 um
2.00 MeV	1.253E+00	7.726E-04	977.05 um	39.83 um	59.85 um

Multiply Stopping by	for Stopping Units
1.0000E-01	eV / Angstrom
1.0000E+00	keV / micron
1.0000E+00	MeV / mm
1.0000E-01	keV / (ug/cm2)
1.0000E-01	MeV / (mg/cm2)
1.0000E+02	keV / (mg/cm2)
3.3191E+00	eV / (1E15 atoms/cm2)
1.9438E+00	L.S.S. reduced units

Appendix C

Thermal Calculations:

1. TEMPERATURE GRADIENT

Energy per Proton * Current * Proton per Charge = Power

$$\frac{1MeV}{H+}\frac{10^6 eV}{1MeV}\frac{1.6*10^{-19} Joules}{eV}\frac{10^{-7} Coulombs}{\text{sec}}\frac{H+}{1.6*10^{-19} Coulombs} = 0.1 Watts$$

$$H = -kA\frac{dT}{dx} \qquad (1)$$

Current = 0.1 μA

Aerogel Thickness = 1 mm

H = the Heat Transferred in a time t

- Assume all the power of the bombarding particles is going into Heat Transfer

k = Thermal Conductivity = 0.007 milliwatts/ m-K

A= Cross Sectional Area of Aerogel = 10^{-4} m^2

$\frac{dT}{dx}$ = the change in temperature (K) over a distance x (m)

$$\frac{dT}{dx} = -\frac{H}{kA} = -\frac{143K}{\mu m}$$

2. STEFAN-BOLTZMAN LAW

$$P = \sigma A e T^4 \qquad (2)$$

σ = Stefan's constant = 5.67 * 10^{-8} W/ m^2 - K^4

A= Surface Area of Aerogel = 2*10^{-4} m^2

e = emissivity (0.8 for silica brick)

T = Temperature (K)

- Assume Aerogel is in thermal equilibrium at temperature T, radiating energy at the same rate it is absorbing

$0.1\ W = 5.67 * 10^{-8}\ W/m^2 - K^4 * 2*10^{-4}\ m^2 * 0.8 * T^4$

- e value of a Silica brick is 0.8--although aerogels are SiO_2, they probably have lower emissivities than a typical silica brick, which would mean higher temperatures in thermal equilibrium.

T = <u>324 K</u>

- The temperature of the aerogel may be higher when it is not in thermal equilibrium (most likely during initial bombardment)

If the emissivity of an aerogel was closer to 0.2, T will be 815 K.

- Temperatures could be much higher than 324 K

3. SPECIFIC HEAT

$$Q = mc\Delta T \qquad (3)$$

- Assume all of energy going into aerogel is in the form of heat
- Assume aerogel has a specific heat similar to water

After 10 seconds, Q = 1 Joule

$m = (0.1\ grams / cm^3) * (0.1\ cm^3) = 0.01\ grams = 10^{-5}\ kg$

c = 4186 J/ kg-C° (specific heat of water)

$\Delta T = 24\ C° =$ <u>24 K</u>

- If it was assumed the aerogel had a specific heat closer to glass, it could change in temperature by up to 120 K in 10 seconds.

Works Cited

"Aerogels: Solid Pieces of Nothing" Compressed Air Magazine. June 1989, pgs 27-31.

Anderson, K.J. "From Aquagels to Aerogels" MRS Bulletin. March 1991, pg 63-64.

Anderson, H. H. and Ziegler, J.F. Hydrogen: Stopping Powers and Ranges in all Elements. Pergamon Press, New York: 1977

Bashkin, S., ed. Beam-Foil Spectroscopy: Proceedings of the Conference on Beam-Foil Spectroscopy held at the University of Arizona, Nov. 20-22, 1967. Gordon and Breach, New York: 1968.

Biersack, J.P and Ziegler, J.F. Simulation Computer Program: TRIM (Transport and Range of Ions through matter). 1989.

CRC Handbook of Chemistry and Physics, 56th edition. CRC Press, Cleveland: 1975.

HEM Data Corporation: PC-Based Testing and Analysis Products. Snap Master User Guide. HEM Data Corp., Southfield, Michigan: 1994.

Hunt, A. J. "Aerogels: The Lightest Solids" Chapter of the Encyclopedia Britannica 1995 Science Year Book.

Instruction Manual HVI-475M1: The Model AN-2000 Positive Ion Accelerator. HV Engineering: Burlington, n.d.

Leverenz, H.W. An Introduction to Luminescence of Solids. Dover Publications, New York: 1968.

Morrison, R. Spectral Characteristics of an Aerogel. University of Arizona M.S. Thesis: 1995.

Scanning Monochrometer EU-700 and EUE-700 Series. Benton Harbor, Heath: 1979.

Serway, R. A. Physics for Scientists and Engineers. Saunders College Publishing, Philadelphia: 1990.

Thornton, S.T. and Rex, A. Modern Physics for Scientists and Engineers. Saunders College Publishing, Fort Worth, Tx.: 1993.

Wu, Corrina. Aerogel Films as Electronic Insulators. Science News, Vol 150. Dec. 1996, pg 383.